

# Multiplicity of Galactic Cepheids from long-baseline interferometry

## IV. New detected companions from MIRC and PIONIER observations<sup>\*</sup>

A. Gallenne<sup>1,2</sup>, P. Kervella<sup>3</sup>, S. Borgniet<sup>3</sup>, A. Mérand<sup>4</sup>, G. Pietrzyński<sup>5</sup>, W. Gieren<sup>6,7</sup>, J. D. Monnier<sup>8</sup>, G. H. Schaefer<sup>9</sup>, N. R. Evans<sup>10</sup>, R. I. Anderson<sup>4</sup>, F. Baron<sup>8,11</sup>, R. M. Roettenbacher<sup>12,8</sup> and P. Karczmarek<sup>13</sup>

<sup>1</sup> European Southern Observatory, Alonso de Córdova 3107, Casilla 19001, Santiago, Chile

<sup>2</sup> Laboratoire Lagrange, UMR7293, Université de Nice Sophia-Antipolis, CNRS, Observatoire de la Côte d'Azur, Nice, France

<sup>3</sup> LESIA, Observatoire de Paris, CNRS UMR 8109, UPMC, Université Paris Diderot, 5 Place Jules Janssen, F-92195 Meudon, France

<sup>4</sup> European Southern Observatory, Karl-Schwarzschild-Str. 2, 85748 Garching, Germany

<sup>5</sup> Nicolaus Copernicus Astronomical Centre, Polish Academy of Sciences, Bartycka 18, PL-00-716 Warszawa, Poland

<sup>6</sup> Universidad de Concepción, Departamento de Astronomía, Casilla 160-C, Concepción, Chile

<sup>7</sup> Millennium Institute of Astrophysics, Santiago, Chile

<sup>8</sup> Astronomy Department, University of Michigan, Ann Arbor, MI 48109, USA

<sup>9</sup> The CHARA Array of Georgia State University, Mount Wilson CA 91023, USA

<sup>10</sup> Smithsonian Astrophysical Observatory, MS 4, 60 Garden Street, Cambridge, MA 02138, USA

<sup>11</sup> Department of Physics and Astronomy, Georgia State University, Atlanta, GA 30303, USA

<sup>12</sup> Yale Center for Astronomy and Astrophysics, Department of Physics, Yale University, New Haven, CT, 06520 USA

<sup>13</sup> Obserwatorium Astronomiczne, Uniwersytet Warszawski, Al. Ujazdowskie 4, 00-478, Warsaw, Poland

December 27, 2018

### ABSTRACT

**Aims.** We aim at detecting and characterizing the main-sequence companions of a sample of known and suspected Galactic binary Cepheids. The long-term objective is to accurately and independently measure the Cepheid masses and the distances.

**Methods.** We used the multi-telescope interferometric combiners CHARA/MIRC and VLTI/PIONIER to detect and measure the astrometric positions of the high-contrast companions orbiting 16 bright Galactic Cepheids. We made use of the CANDID algorithm to search for the companions and set detection limits from interferometric observations. We also present new high-precision radial velocity measurements which were used to fit radial pulsation and orbital velocities.

**Results.** We report the detection of the companions orbiting the Cepheids U Aql, BP Cir, and S Mus, possible detections for FF Aql, Y Car, BG Cru, X Sgr, V350 Sgr, and V636 Sco, while no component is detected around U Car, YZ Car, T Mon, R Mus, S Nor, W Sgr and AH Vel. For U Aql and S Mus, we performed a preliminary orbital fit combining their astrometric measurements with newly obtained high-precision single-line radial velocities, providing the full set of orbital elements and pulsation parameters. Assuming the distance from a period-luminosity (P-L) relation for both Cepheids, we estimated preliminary masses of  $M_{U\text{Aql}} = 4.97 \pm 0.62 M_{\odot}$  and  $M_{S\text{Mus}} = 4.63 \pm 0.99 M_{\odot}$ . For YZ Car, W Sgr, V350 Sgr, and V636 Sco, we revised the spectroscopic orbits using new high-precision radial velocities, while we updated the pulsation parameters for BP Cir, BG Cru, S Nor and AH Vel. Our interferometric observations also provide measurements of the angular diameters, that can be used in a Baade-Wesselink type analysis.

**Conclusions.** We have now several astrometric detections of Cepheid companions. When radial velocities of the companions will be available, such systems will provide accurate and independent masses and distances. Orbital parallaxes with an accuracy better than 5% will be particularly useful for a better calibration of the P-L relation. The final Gaia parallaxes will be also particularly helpful for single-line spectroscopic systems, where mass and distance are degenerate. Mass measurements are necessary for a better understanding of the age and evolution of Cepheids.

**Key words.** techniques: interferometric – techniques: high angular resolution – stars: variables: Cepheids – star: binaries: close

## 1. Introduction

Classical Cepheids are mainly known as primary distance indicators in the local Universe thanks to the period-luminosity relation discovered about a century ago (Leavitt 1908; Leavitt & Pickering 1912). Moreover, these pulsating intermediate-mass stars provide fundamental constraints for studying pulsation and evolution models (see e.g. Anderson et al. 2016b; Gillet 2014; Neil-

son & Ignace 2014; Prada Moroni et al. 2012; Bono et al. 2006). Now with the actual precise photometric and spectroscopic instruments, finer structures of Cepheids are being revealed (see e.g. Derekas et al. 2017; Evans et al. 2015; Anderson 2014), providing new information on these standard candles. Yet, despite all instrument improvements, direct measurements of the most fundamental stellar property, the mass, are still missing for most of the Cepheids. It is necessary to obtain an accurate and model-independent estimate of this parameter as the overall lifetime and behaviour of a star is determined primarily by its mass. Measurements of Cepheid masses are even more critical to constrain the long-standing mass discrepancy problem,

Send offprint requests to: A. Gallenne

<sup>\*</sup> Based on observations made with ESO telescopes at Paranal and La Silla observatory under program IDs 091.D-0041, 094.D-0170, 190.D-0237(A) and 091.D-0469(A).

still not really understood. The most cited scenarios to explain this discrepancy between masses predicted by stellar evolutionary and pulsation models are a mass-loss mechanism during the Cepheid's evolution, convective core overshooting, and rotation during the main-sequence stage (Anderson et al. 2014; Neilson et al. 2011; Keller 2008; Bono et al. 2006).

Cepheid masses are usually derived through the companion mass which is itself inferred from a mass-temperature relation. The estimated masses are therefore model-dependent. A few dynamical masses of Cepheids were measured in the Large Magellanic Cloud from eclipsing binary systems (Pilecki et al. 2018; Gieren et al. 2014; Pilecki et al. 2013; Pietrzyński et al. 2010), and already provide some insight to settle the discrepancy between pulsation and evolution models. In our Galaxy, only the mass of Polaris and V1334 Cyg has been measured through the combination of astrometric and spectroscopic measurements of its close companion (Gallenne et al. 2018a; Evans et al. 2018a, 2008). Otherwise, all companions were detected from the orbital effects on the radial velocities (RVs) and the variability of the systemic velocity, which provided the first information about the orbits. However, only massive and close components can be detected this way (see e.g. Moore 1929; Abt 1959; Szabados 1989, 1991). Spectra from the International Ultraviolet Explorer (IUE) also provided useful information such as the spectral type of some companions (see e.g. Böhm-Vitense & Proffitt 1985; Evans 1992a), but this also suffers from observational bias as only UV bright companions can be detected. However, UV wavelengths seem to be the best option to detect lines from the orbiting companions as most of them are main-sequence B stars, although the task is complicated as they are often fast rotators with very broad lines. At longer wavelengths, the Cepheid brightness outshines the companion, making challenging any detection with the current available instruments.

Recently, Kervella et al. (2018) searched for close-in companions from the signature of their orbital motion on the proper motion vector, i.e. by comparing the Hipparcos and Gaia proper motions (PMs) to the mean PM. This work revealed a significant number of new candidate companions, and indicated a high binarity fraction (close to 100%). For some of them with a known spectroscopic orbit, the combination of the PM and the distance (assumed from a P-L relation) allowed the determination of the full set of orbital elements. With an assumed mass for the Cepheids, it also provides approximate masses of their companions.

Another issue in detecting Cepheid companions is the angular separation ( $\lesssim 50$  mas) which makes difficult the detection from high-contrast imaging instruments. Adaptive-optics (AO) works in the infrared, and the flux ratio,  $f$ , at these wavelengths between the companion and the Cepheid is only a few percent ( $f < 1\%$  in most cases), making impossible to directly detect faint components located within 100 milliarcseconds (mas). A few wider companions, however, can be spatially resolved with or without AO, as demonstrated by Gallenne et al. (2014a) and Evans et al. (2013). A possible solution to detect such faint components in the separation range  $50 < r < 100$  mas would be to use aperture masking, which can yield contrast  $\Delta K \sim 6$  mag at  $\lambda/D$  (Kraus & Ireland 2012). The best technique for  $r \lesssim 50$  mas is long-baseline interferometry (LBI), which can reach contrast  $\Delta H \sim 6$  mag. Gallenne et al. (2015, 2014b, 2013) proved the efficiency of LBI by detecting close faint companions of Cepheids, down to  $\Delta H = 5.3$  mag ( $f = 0.8\%$ , Gallenne et al. 2014b). Gallenne et al. (2015) also detected a companion as faint as  $f = 0.22\%$ , which is the faintest companion detected so far by interferometry, but still needs to be confirmed.

The advantage of spatially resolving binary Cepheids lies in the combination of the astrometric and spectroscopic measurements which provides an independent and reliable way to determine stellar masses and distances. But the mass and the distance are degenerate parameters if the system is not a double-line spectroscopic binary. This is the case for most of the binary Cepheids as usually RV measurements are made in the  $V$  band, and only provide RVs of the Cepheid (the primary). As mentioned previously, RV measurements in the UV are more favourable to detect lines of the companions, and combining such observations with astrometry will provide both the Cepheid mass and distance. However, broad features (many are fast rotators) and blended lines in the spectra of the companions complicate the analysis, and prevent the determination of accurate RVs. In a recent work, we succeeded in determining RVs of the companion orbiting the Cepheid V1334 Cyg using the Space Telescope Imaging Spectrograph (STIS) on board the Hubble Space Telescope (HST). This work provides the most accurate distance for a Cepheid at a 1% accuracy level, and masses with 3% accuracy (Gallenne et al. 2018a). For systems where RVs measurements of the companions are still not possible, the future Gaia parallaxes will allow us to break the degeneracy between mass and distance, and we will then be able to combine interferometry with single-line velocities to estimate dynamical masses of many Cepheids.

We are engaged in a long-term interferometric observing program to detect and follow-up close faint companions orbiting the brightest Galactic Cepheids. This program already provided new information for four Cepheids and their respective companions (Gallenne et al. 2015, 2014b, 2013). We are also engaged in an ultraviolet and visible spectroscopic observing campaign which aims at detecting the companion lines and measured contemporaneous high-precision RVs.

In this fourth paper, we report new interferometric observations of 16 Galactic Cepheids. We used the multi-telescope combiners CHARA/MIRC and VLTI/PIONIER which offer the best  $(u, v)$  coverage and sensitivity to detect faint companions in both the northern and southern hemisphere. The observations and data reduction are described in Sect. 2. In Sect. 3, we used the CANDID<sup>1</sup> tool (Gallenne et al. 2015) to search for companions using all available observables and then derive the detection sensitivity. We discuss our results for each individual binary Cepheid in Sect. 4, in which we also analyse new high-precision RV measurements. We conclude in Sect. 5.

## 2. Observation and data reduction

To spatially resolve faint companions, we need a high-precision multi-telescope recombiner. High-precision because the variations in the signal caused by a faint component have a small amplitude, while using several telescopes gives much more simultaneous measurements to properly cover the  $(u, v)$  plane, and improve the observing efficiency considerably. For this purpose we used the CHARA/MIRC and VLTI/PIONIER combiners, allowing us to observe Cepheids in both hemispheres.

### 2.1. Northern interferometric observations

The observations were performed with the Michigan InfraRed Combiner (MIRC) installed at the CHARA array (ten Brummelaar et al. 2005), located on Mount Wilson, California. The CHARA array consists of six 1 m aperture telescopes with an Y-shaped configuration (two telescopes on each branch), oriented

<sup>1</sup> Available at <https://github.com/amerand/CANDID>

**Table 1.** Journal of the observations.

Star	UT	Instrument	Configuration	$N_{sp}$	$N_{V^2}, N_{CP}$	Calibrators
U Aql	2012 Jul. 27	MIRC	S1-S2-E2-W1-W2	8	1088, 662	HD185124, HD198001
	2013 Sep. 14	MIRC	S1-S2-E2-W1-W2	8	560, 511	HD184985, HD196870
	2016 Jul. 20	MIRC	S1-S2-E2-W1-W2	8	1337, 1594	HD177067, HD178218, HD188844
FF Aql	2012 Jul. 26	MIRC	S1-S2-E1-E2-W1-W2	8	1496, 2000	HD166230, HD182807
U Car	2016 Mar. 07	PIONIER	A0-G1-J2-J3	6	1018, 483	HD96068, HD98897, HD100078
	2017 Mar. 21	PIONIER	A0-G1-J2-K0	6	1950, 1561	HD98692, HD98732, HD99048
	2017 Jun. 27	PIONIER	A2-D0-J3-K0	6	583, 475	HD90074, HD90980, HD98897
Y Car	2016 Mar. 06	PIONIER	A0-G1-J2-J3	6	573, 362	HD93307, HD92156, HD89839
YZ Car	2016 Mar. 05	PIONIER	A0-G1-J2-J3	6	898, 458	HD90246, HD89517, HD85253
	2016 Mar. 06	PIONIER	A0-G1-J2-J3	6	817, 524	HD97744, HD94256
BP Cir	2015 Feb. 17	PIONIER	A1-G1-J3-K0	6	1620, 1080	HD130551, HD132209, HD121901
BG Cru	2016 Mar. 04	PIONIER	A0-G1-J2-J3	6	807, 556	HD110532, HD110924, HD115669
T Mon	2016 Dec. 27	PIONIER	A0-G1-J2-J3	6	323, 240	HD43299, HD45317
	2017 Jan. 06	PIONIER	A0-G1-J2-K0	6	360, 240	
R Mus	2016 Mar. 07	PIONIER	A0-G1-J2-J3	6	1060, 705	HD109761, HD101805, HD125136
S Mus	2015 Feb. 16	PIONIER	A1-G1-J3-K0	6	1980, 1320	HD107013, HD109761, HD102969
	2016 Mar. 05	PIONIER	A0-G1-J2-J3	6	1046, 689	HD112124, HD105939, HD107720
	2017 Mar. 04	PIONIER	A0-G1-J2-J3	6	1440, 960	HD102534, HD105939, HD107720
S Nor	2016 Mar. 05	PIONIER	A0-G1-J2-J3	6	1251, 833	HD147075, HD148679, HD151005
	2017 May 27	PIONIER	B2-D0-J3-K0	6	872, 584	HD146247, HD145361, HD148679
	2017 Jun. 22	PIONIER	A0-G1-J2-J3	6	1912, 1302	HD147422, HD144230, HD145883
W Sgr	2017 Jun. 23	PIONIER	A0-G1-J2-J3	6	1094, 1595	HD162415, HD163652, HD169236
X Sgr	2017 May 27	PIONIER	B2-D0-J3-K0	6	540, 360	HD157919, HD156992, HD166295
V350 Sgr	2013 Jul. 10	PIONIER	A1-G1-J3-K0	3	630, 392	HD174774, HD171960
	2013 Jul. 14	PIONIER	D0-G1-H0-I1	3	821, 546	
V636 Sco	2017 Jun. 22	PIONIER	A0-G1-J2-J3	6	409, 201	HD174423
	2013 Jul. 10	PIONIER	A1-G1-J3-K0	3	322, 311	HD154486, HD159941
	2015 Feb. 16	PIONIER	A1-G1-J3-K0	6	936, 237	HD151337, HD159217, HD160113
	2016 Mar. 06	PIONIER	A0-G1-J2-J3	6	1183, 307	HD149835, HD152272, HD155019
	2016 Mar. 07	PIONIER	A0-G1-J2-J3	6	672, 312	
	2017 May 27	PIONIER	B2-D0-J3-K0	6	377, 582	HD154250, HD159285, HD155019
	2017 May 27	PIONIER	B2-D0-J3-K0	6	377, 582	HD154250, HD159285, HD155019
AH Vel	2016 Dec. 28	PIONIER	A0-G1-J2-J3	6	191, 195	HD66080, HD70195, HD73075
	2017 Jan. 01	PIONIER	A0-G1-J2-J3	6	1044, 696	
	2017 Jan. 27	PIONIER	A0-G1-J2-J3	6	828, 552	

**Notes.**  $N_{V^2}$  and  $N_{CP}$ : total number of squared visibilities and closure phases.  $N_{sp}$ : number of spectral channels. Adopted calibrator diameters are listed in Table A.1.

to the east (E1, E2), west (W1, W2) and south (S1, S2), providing a good coverage of the  $(u, v)$  plane. The baselines range from 34 m to 331 m, providing a high angular resolution down to  $\sim 0.5$  mas in  $H$ . The MIRC instrument (Monnier et al. 2004, 2010) is an image-plane combiner which enables us to combine the light coming from all six telescopes in  $K$  or  $H$ . MIRC also offers three spectral resolutions ( $R = 42, 150$  and  $400$ ), which provide 15 visibility and 20 closure phase measurements across a range of spectral channels.

We observed the Cepheids FF Aql (HD 176155,  $P_{puls} = 4.47$  d) and U Aql (HD 183344,  $P_{puls} = 7.02$  d) with five and six telescopes. We used the  $H$ -band filter with the lowest spectral resolution, where the light is split into eight spectral channels. Table 1 lists the journal of our observations. We followed a standard observing procedure, i.e. we monitored the interferometric transfer function by observing a calibrator before and/or after our Cepheids. The calibrators, listed in Table 1, were selected using the *SearchCal*<sup>2</sup> software (Bonneau et al. 2006, 2011) provided by the Jean-Marie Mariotti Center (JMMC).

We reduced the data using the standard MIRC pipeline (Monnier et al. 2007), which consists of computing the squared

visibilities and triple products for each baseline and spectral channel, and to correct for photon and readout noises. Squared visibilities are estimated using Fourier transforms, while the triple products are evaluated from the amplitudes and phases between three baselines forming a closed triangle.

## 2.2. Southern interferometric observations

We used the Very Large Telescope Interferometer (VLTI ; Haguenaer et al. 2010) with the four-telescope combiner PIONIER (Precision Integrated Optics Near-infrared Imaging Experiment, Le Bouquin et al. 2011) to measure squared visibilities and closure phases of the southern binary systems. PIONIER combines the light coming from four telescopes in the  $H$  band, either in a broad band mode or with a low spectral resolution, where the light is dispersed across six spectral channels (three before December 2014). The recombination provides simultaneously six visibilities and four closure phase signals per spectral channel.

Our observations were carried out from 2013 to 2017 using the 1.8 m Auxiliary Telescopes with the largest available configurations, providing six projected baselines ranging from 40

<sup>2</sup> Available at <http://www.jmmc.fr/searchcal>.

to 140 m. PIONIER was setup in *GRISM* mode, i.e. the fringes are dispersed into six spectral channels (three before December 2014). As for MIRC, we monitored the interferometric transfer function with the standard procedure which consists of interleaving the science target by reference stars. The calibrators were also selected using the *SearchCal* software, and are listed in Table 1, together with the journal of the observations.

The data have been reduced with the *pndrs* package described in Le Bouquin et al. (2011). The main procedure is to compute squared visibilities and triple products for each baseline and spectral channel, and to correct for photon and readout noises.

### 3. Companion search and sensitivity limit

We used the CANDID code developed by Gallenne et al. (2015), which is a set of Python tools allowing us to search systematically for companions and estimate the detection limit using all interferometric observables. Briefly, the first main function of CANDID performs a 2D grid of fit using a least-squares algorithm. At each starting position, the companion position, its flux ratio and the angular diameters (if components are spatially resolved) are fitted. CANDID also includes a tool to estimate the detection level of the companion in number of sigmas (assuming the error bars in the data are uncorrelated). Uncertainties on the fitted parameters are estimated using a bootstrapping function. From the distribution, we took the median value and the maximum value between the 16th and 84th percentiles as uncertainty for the flux ratio and the angular diameter. For the fitted astrometric position, the error ellipse is derived from the bootstrap sample (using a principal components analysis). The second main function incorporates a robust method to set a  $3\sigma$  detection limit on the flux ratio for undetected components, which is based on an analytical injection of a fake companion at each point in the grid. We refer the reader to Gallenne et al. (2015) for more details about CANDID.

Because of spectral smearing across one spectral channel, we searched for companions with a maximum distance to the main star of 50 mas. The spectral smearing field of view (FoV) is defined by  $\lambda^2/(B\Delta\lambda)$ , where  $\lambda$  is the wavelength of the observations,  $\Delta\lambda$  the width of the spectral channels, and  $B$  the interferometric baseline. For our observation, we have limited our search within 50 mas, although the CANDID algorithm includes an analytical model to avoid significant smearing.

In the following, we search for companions using either all observables (i.e. the squared visibilities  $V^2$ , the bispectrum amplitudes  $B_{\text{amp}}$ , and the closure phases  $CP$ ) or only the closure phases. As explained by Gallenne et al. (2015), the  $CP$  is more sensitive to faint off-axis companions (although depending on its location and the  $(u, v)$  coverage) and is also less affected by instrumental and atmospheric perturbations than the other observables. Fitting all of the observables can improve the detection level because we add more information, but it can also affect the results, depending on the magnitude of the biases altering the  $V^2$  data. The detection of a companion is claimed if the significance level is  $> 3\sigma$  and consistent between observables.

Although CANDID has implemented two methods to derive the sensitivity limits, we only listed the ones given by the injection method, which has been proven to be more robust for biased data (see Gallenne et al. 2015).

In this section we present the results of the companion search for each individual stars. A detailed discussion is presented in Sect. 4 for detected and non-detected components.

#### 3.1. U Aql

This 7.02 d period Cepheid has been studied for decades using visible spectroscopy (see e.g. Sanford 1930; Szabados 1989; Wilson et al. 1989; Bersier 2002). It is a well known spectroscopic binary with an orbital period of 1856.4 d, first discovered by Slovak et al. (1979), and then confirmed with the determination of the orbital elements by Welch et al. (1987). Observations using the IUE also detected the presence of a hot companion (Böhm-Vitense & Proffitt 1985; Evans 1992b), from which a spectral type of B9.8V has been estimated. This would correspond to a flux ratio  $\sim 0.45\%$ <sup>3</sup> (mean value as it also depends on the pulsation phase of the Cepheid). According to the orbital elements and the estimate of the orbital inclination by Welch et al. (1987,  $i = 74^\circ$ , using the mass function and the assumed masses  $7 M_\odot$  for U Aql and  $2 M_\odot$  for its companion), the projected semi-major axis is expected to be  $\sim 9$  mas. This value is consistent with the 9.5 mas estimate of Kervella et al. (2018) using the values of the spectroscopic orbit and the proper motion vectors (and assuming a mass of  $5.2 M_\odot$  for the Cepheid). The available baselines at CHARA allow us to spatially resolve such separation.

We obtained three measurement epochs spread over four years, and a companion is detected at each epoch. For the first observations, the seeing conditions were poor at  $\sim 1.3''$ . We noticed that including  $B_{\text{amp}}$  leads to the detection of a companion which is too bright ( $f \sim 2.5\%$ ), and is not consistent with the detection using  $CP + V^2$  or only  $CP$ , which give the exact same position and flux ratio. We therefore decided to not use this observable which is more affected by the atmospheric conditions. The detections using the  $CP$ s only and  $CP + V^2$  give similar levels,  $3.1\sigma$  and  $2.8\sigma$  respectively. For the second epoch, the atmospheric conditions were better ( $\sim 0.7''$ ), and a companion is detected at more than  $5\sigma$  in all observables. For the last epoch, the detection level ranges between 1.5 and  $2.9\sigma$ . Although the significance level is low, the detection is well localized and the derived flux ratio seems consistent with our previous observations. The values are listed in Table 2. Although additional observations are necessary to confirm, a tentative orbital fit is discussed in Sect. 4.

As previously explained, we estimate the  $3\sigma$  sensitivity limits with CANDID (i.e. by injecting fake companions with various flux ratio at all azimuth), to detect a possible third component by analytically removing the detected companion for all epochs (see Gallenne et al. 2015). In Table 3, we calculated conservative values corresponding to the mean plus the standard deviation for the given radius ranges  $r < 25$  mas and  $r < 50$  mas. We found no companion with a flux ratio higher than 0.6% within 50 mas.

We also measured the angular diameter for a uniform disk model, its value is reported in Table 2. We estimated the uncertainty by using the conservative formalism of Boffin et al. (2014):

$$\sigma_{\theta_{\text{UD}}}^2 = N_{\text{sp}}\sigma_{\text{stat}}^2 + \delta\lambda^2\theta_{\text{UD}}^2 \quad (1)$$

where  $N_{\text{sp}}$  is the number of spectral channels. The first term takes into account that the spectral channels are almost perfectly correlated, and  $\delta\lambda = 0.0025$  or  $0.0035$ , coming from the fact that the absolute wavelength calibration is precise at a 0.25% level for MIRC (Monnier et al. 2012) and 0.35% for PIONIER (Gallenne et al. 2018b; Kervella et al. 2017).  $\sigma_{\text{stat}}$  is the statistical

<sup>3</sup> Converted using the grid of Pecaut & Mamajek (2013) (see also Pecaut et al. 2012 and [http://www.pas.rochester.edu/~emamajek/EEM\\_dwarf\\_UBVIJHK\\_colors\\_Teff.txt](http://www.pas.rochester.edu/~emamajek/EEM_dwarf_UBVIJHK_colors_Teff.txt)) and the average Cepheid magnitudes (Storm et al. 2011; van Leeuwen et al. 2007).

**Table 2.** Final best-fit parameters.

#	Star	MJD (day)	$\phi$	$\theta_{\text{UD}}$ (mas)	$f$ (%)	$\Delta\alpha$ (mas)	$\Delta\delta$ (mas)	$\sigma_a$ (mas)	$\sigma_b$ (mas)	$\sigma_{\text{PA}}$ ( $^\circ$ )	All	$n\sigma$ CP
1	U Aql	56135.316	0.11	$0.706 \pm 0.042$	$0.74 \pm 0.15$	-4.855	-0.874	0.111	0.068	99.7	2.8	3.1
2		56549.230	0.04	$0.792 \pm 0.027$	$0.44 \pm 0.09$	3.798	-8.948	0.075	0.056	-52.7	5.8	6.1
3		57589.297	0.11	$0.786 \pm 0.042$	$0.73 \pm 0.32$	-2.709	6.564	0.161	0.048	68.2	2.9	2.2
4	FF Aql	56134.252	0.11	$0.834 \pm 0.014$	$0.56 \pm 0.29$	1.167	8.787	0.100	0.090	40.8	1.9	1.2
5	U Car	57455.099	0.85	$0.909 \pm 0.011$	-	-	-	-	-	-	1.3	2.8
6		57834.138	0.61	$0.948 \pm 0.024$	-	-	-	-	-	-	1.2	1.1
7		57901.017	0.35	$0.825 \pm 0.037$	-	-	-	-	-	-	1.1	2.2
8	Y Car	57454.082	0.42	$0.19 \pm 0.10$	$0.94 \pm 0.10$	2.440	0.392	0.323	0.070	68.2	6.3	2.4
9	YZ Car	57453.111	0.13	$0.367 \pm 0.036$	-	-	-	-	-	-	2.7	1.3
10		57454.157	0.19	$0.372 \pm 0.033$	-	-	-	-	-	-	2.1	2.9
9+10		-	-	0.370	-	-	-	-	-	-	-	2.7
11	BP Cir	57071.327	0.59	$0.254 \pm 0.125$	$3.24 \pm 0.21$	11.097	34.525	0.058	0.053	-16.5	> 50	> 50
12	BG Cru	57452.399	0.11	$0.694 \pm 0.028$	$0.53 \pm 0.12$	1.981	6.352	0.238	0.097	-66.8	2.3	4.5
13	T Mon	57750.185	0.79	$0.904 \pm 0.016$	-	-	-	-	-	-	2.9	2.8
14		57760.259	0.16	$0.703 \pm 0.093$	-	-	-	-	-	-	2.3	1.3
13+14		-	-	0.803	-	-	-	-	-	-	-	2.0
15	R Mus	57455.169	0.31	$0.457 \pm 0.023$	-	-	-	-	-	-	0.9	1.6
16	S Mus	57070.277	0.17	$0.560 \pm 0.034$	$0.86 \pm 0.03$	0.648	2.297	0.117	0.026	99.6	21.2	> 50
17		57453.206	0.81	$0.599 \pm 0.027$	$1.09 \pm 0.09$	3.037	-0.804	0.108	0.060	68.5	25	22
18		57817.174	0.49	$0.677 \pm 0.033$	$0.80 \pm 0.11$	-0.496	-2.394	0.218	0.133	55.2	5.7	7.4
19	S Nor	57453.297	0.35	$0.639 \pm 0.020$	-	-	-	-	-	-	1.8	2.2
20		57901.172	0.26	$0.661 \pm 0.039$	-	-	-	-	-	-	1.7	1.5
21		57927.113	0.92	$0.511 \pm 0.040$	-	-	-	-	-	-	2.3	1.3
20+21		-	-	0.586	-	-	-	-	-	-	-	1.3
22	W Sgr	57928.170	0.23	$1.079 \pm 0.023$	-	-	-	-	-	-	2.7	1.7
23	X Sgr	57901.305	0.96	$1.250 \pm 0.026$	$0.43 \pm 0.10$	-11.801	-7.704	0.628	0.122	58.3	2.4	5.8
24	V350 Sgr	56484.247	0.90	$0.452 \pm 0.039$	$0.62 \pm 0.12$	0.680	2.949	0.470	0.126	59.6	4.1	1.5
25		56488.126	0.65	$0.515 \pm 0.044$	$0.50 \pm 0.09$	0.563	2.845	0.454	0.181	-50.8	5.4	4.5
24+25		-	-	0.480	$0.55 \pm 0.11$	0.862	2.483	0.184	0.115	-25.1	-	4.1
26		57927.193	0.86	$0.428 \pm 0.022$	-	-	-	-	-	-	1.5	1.5
27	V636 Sco	56484.157	0.65	$0.533 \pm 0.012$	-	-	-	-	-	-	1.4	2.3
28		57070.380	0.90	$0.530 \pm 0.012$	-	-	-	-	-	-	1.3	2.5
29		57454.321	0.38	$0.583 \pm 0.012$	-	-	-	-	-	-	1.3	2.9
30		57455.328	0.53	$0.566 \pm 0.016$	-	-	-	-	-	-	2.2	1.2
29+30		-	-	0.575	-	-	-	-	-	-	-	1.7
31		57901.416	0.16	$0.53 \pm 0.10$	$1.04 \pm 0.58$	-6.594	4.591	0.488	0.039	38.4	3.8	3.6
32	AH Vel	57751.103	0.21	$0.343 \pm 0.051$	-	-	-	-	-	-	1.0	2.3
33		57755.265	0.20	$0.456 \pm 0.038$	-	-	-	-	-	-	0.8	1.2
34		57781.183	0.33	$0.408 \pm 0.049$	-	-	-	-	-	-	1.4	1.0
32+33+34		-	-	0.402	-	-	-	-	-	-	-	1.4

**Notes.** MJD: modified Julian date.  $\phi$ : pulsation phase, calculated with the ephemeris listed in Table 4 to 11 for U Aql, FF Aql, YZ Car, BP Cir, BG Cru, S Mus, S Nor, W Sgr, V350 Sgr, V636 Sco and AH Vel, and from Samus et al. (2017) for U Car, Y Car, T Mon, R Mus and X Sgr.  $\theta_{\text{UD}}$ : uniform disk angular diameter.  $f$ ,  $\Delta\alpha$ ,  $\Delta\delta$ :  $H$ -band flux ratio and relative astrometric position of the companion.  $\sigma_a$ ,  $\sigma_b$ ,  $\sigma_{\text{PA}}$ : uncertainty of the astrometric position expressed by the error ellipse with major and minor axes and the position angle measured from north through east.  $n\sigma$ : detection level in number of sigma when fitting all observables or only the CPs. The listed astrometric positions correspond to the fit with the highest detection level.

**Table 3.**  $3\sigma$  average contrast limits in the  $H$  band using all observables or only the closure phases.

		$\Delta H$ (mag)				Sp. Type		Instrument
		All		CP		upper limit		
		$r < 25$ mas	$r < 50$ mas	$r < 25$ mas	$r < 50$ mas			
U Aql	2012-07-27	4.6	4.3	4.7	4.4	B6V	B3V	MIRC
	2013-09-14	5.8	5.5	5.5	5.5	B9V	B9V	
	2016-07-20	5.5	5.4	5.6	5.2	B9V	B9V	
FF Aql	2012-07-26	5.3	4.8	5.7	5.3	A3V	A0V	MIRC
U Car	2016-03-07	5.7	5.6	6.0	6.0	B2V	B2V	PIONIER
	2017-03-21	4.9	4.6	5.5	5.2	B1V	B1V	
	2017-06-27	5.1	4.8	5.8	5.7	B2V	B2V	
Y Car	2016-03-06	5.1	5.0	4.0	4.0	A0V	A0V	PIONIER
YZ Car	2016-03-05	5.0	5.3	4.6	4.4	B2V	B2V	PIONIER
	2016-03-06	5.2	5.4	4.2	4.4	B2V	B3V	
	combined	–	–	4.8	4.7	B2V	B2V	
BP Cir	2015-02-17	5.0	4.7	4.9	4.6	A6V	A5V	PIONIER
BG Cru	2016-03-04	5.1	4.9	5.3	5.3	A2V	A2V	PIONIER
T Mon	combined	–	–	4.9	4.7	B1V	B1V	PIONIER
R Mus	2016-03-07	4.8	4.4	5.1	5.0	B8V	B8V	PIONIER
S Mus	2015-02-16	4.6	4.2	6.0	5.8	B9V	B9V	PIONIER
	2016 Mar. 05	5.2	5.2	5.1	5.0	B6V	B6V	
	2017 Mar. 04	5.0	4.8	5.0	4.6	B6V	B3V	
S Nor	2016-03-05	5.1	4.8	5.3	5.1	B6V	B5V	PIONIER
	2017 combined	–	–	5.6	5.3	B7V	B5V	
W Sgr	2017-06-23	4.8	4.5	5.2	5.1	B8V	B8V	PIONIER
X Sgr	2017-05-27	4.7	4.4	5.4	5.3	B8V	B8V	PIONIER
V350 Sgr	2013 combined	–	–	5.3	5.0	B9V	B8V	PIONIER
	2017-06-22	4.8	4.9	4.3	4.8	B8V	B8V	
V636 Sco	2013-07-10	5.1	4.9	5.0	4.6	B8V	B8V	PIONIER
	2015-02-02	5.3	5.1	5.6	5.6	B9V	B9V	
	2016 combined	–	–	5.8	5.8	B9V	B9V	
	2017-05-27	5.3	5.2	5.3	5.2	B8V	B8V	
AH Vel	combined	–	–	5.5	5.3	A1V	A0V	PIONIER

error from the bootstrapping technique (bootstrap on the modified Julian date of the calibrated data, with replacement) using 1000 bootstrap samples. We then took from the distributions the median and the maximum value between the 16 % and 84 % percentiles as the uncertainty (although the distributions were roughly symmetrical). We used this formalism for all Cepheids in this paper. Note that the precision of the angular diameter measurement depends on how far down the visibility curve is sampled, so smaller stars will have lower precision.

### 3.2. FF Aql

This Cepheid is possibly a member of a quadruple system, with a spectroscopic and two wide companions. While the spectroscopic component is well known (see e.g. [Abt 1959](#); [Szabados 1977](#); [Evans 1990](#); [Benedict et al. 2007](#)), the existence of the wide companions possibly located at  $\sim 0.2''$  and  $\sim 6.5''$  is more uncertain (for a more detailed discussion of these components see [Gallenne et al. 2014a](#)). From our data, these possible wide companions will not be detected, first because of the spectral smearing FoV, and because of the Gaussian single-mode fiber transmission profile. The spectroscopic component was first discovered by [Abt \(1959\)](#), who derived an orbital period of 1435 days. Additional RVs later enabled us to slightly revise the orbit ([Evans 1990](#); [Gorynya et al. 1998](#)).

Our observations are more suitable to detect this spectroscopic companion, which has a semi-major axis  $a = 12.8$  mas.

This has been derived by [Benedict et al. \(2007\)](#) from binary astrometric perturbations in the Fine Guidance Sensor (FGS) data on board HST. [Evans \(1990\)](#) estimated the companion spectral type to be between A9V and F3V, which give an approximate expected flux ratio in the  $H$  band in the range 0.2-0.4 %. [Fig. 1](#) shows the 2D detection maps given by CANDID, and we see that our MIRC observations did not show any signature of this companion with a detection level  $> 3\sigma$ . We can see a marginal detection at a  $1.9\sigma$  level using all observables, while at  $1.2\sigma$  with the closure phases only. However, although it is not statistically significant, the detection is well localized and the measured flux ratio  $f \sim 0.6\%$  seems fairly consistent with what expected. Additional data are necessary to confirm this detection though. This position of the companion is reported in [Table 2](#), together with the detection levels.

We also derived the  $3\sigma$  sensitivity limits as previously explained, they are listed in [Table 3](#). In [Fig. 2](#) we show this contrast upper limit at  $3\sigma$  using all observables. A maximum contrast of 1:190 is reached within 25 mas. A more detailed discussion is presented in [Sect. 4](#).

### 3.3. U Car

This long-period Cepheid (38.8 d) did not benefit from extensive spectroscopic studies in the past, which is why its binarity was revealed only by [Bersier \(2002\)](#). However, he only detected a  $10 \text{ km s}^{-1}$  offset compared to the previous observations of [Coul-](#)

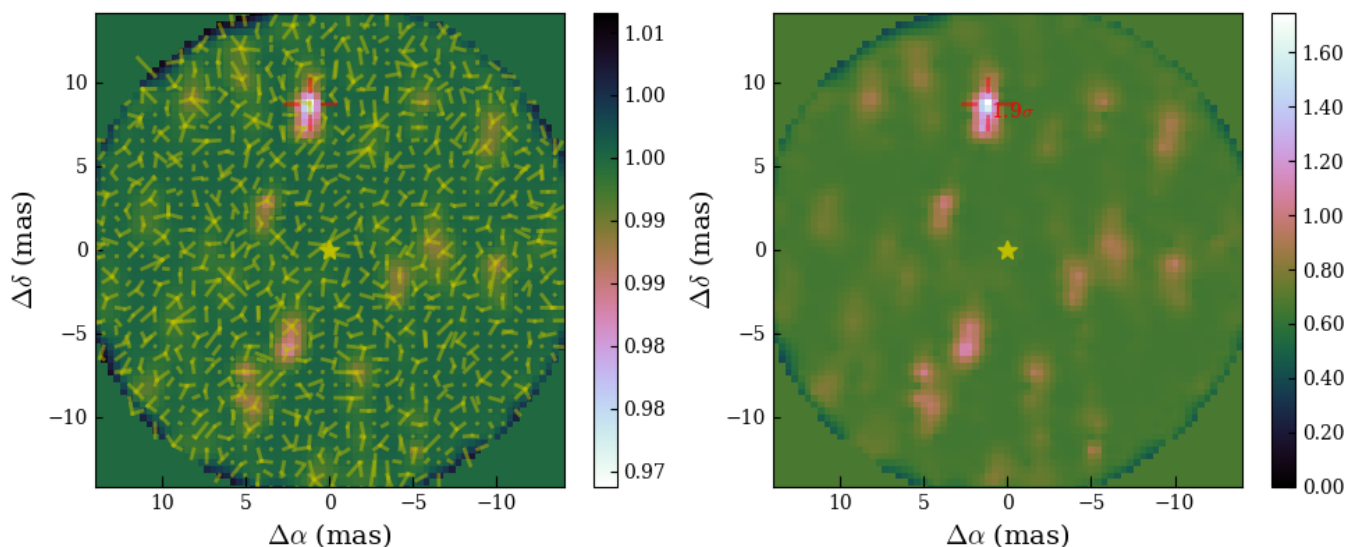


**Fig. 1.**  $\chi^2$  map of the local minima (left) and detection level map (right) of FF Aql using all observables. The yellow lines represent the convergence from the starting points to the final fitted position (for more details see Gallenne et al. 2015). The maps were re-interpolated in a regular grid for clarity. The yellow star denotes the Cepheid.

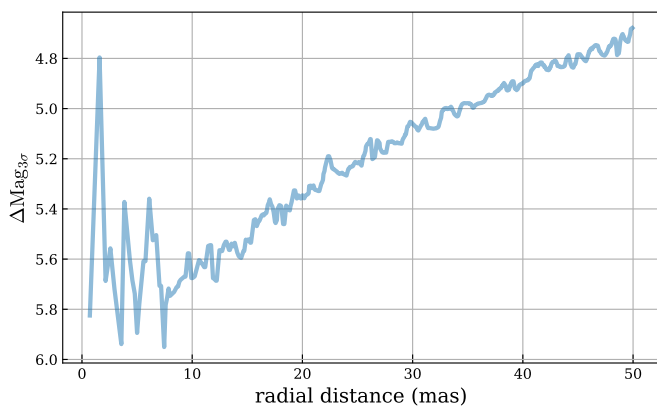


**Fig. 2.**  $3\sigma$  contrast limit for FF Aql.

son & Caldwell (1985), and there is no orbital solution yet. This companion was also not detected by Evans (1992a) from IUE observations, but she derived a spectral type limit for the companion: it has to be later than A1V. This would correspond to a very high contrast of  $\Delta H \gtrsim 8.7$  mag. Note also that Kervella et al. (2018) did not detect a significant anomaly in the PM vectors, suggesting a very long period or a very low mass companion.

We performed three observations with PIONIER spread over approximately one year (see Table 1). Due to the very high contrast of the companion, we do not detect it, our highest detection level being  $2.8\sigma$  (see Table 2). According to our contrast limit listed in Table 3, we were only sensitive to companions with a contrast lower than  $\sim 6$  mag with the best data set.

In Table 2 we also report the angular diameters for a uniform-disk model for each epoch of observations.

### 3.4. Y Car

This short-period double-mode Cepheid is known to be a member of a binary system from the Fourier analysis of the RVs performed by Stobie & Balona (1979a), who could only estimate

a period ranging from 400-600 d because of an incomplete orbital coverage. The full spectroscopic elements were later determined by Balona (1983), and measured an orbital period of  $993 \pm 11$  d. This was then refined by Peterson et al. (2004) to  $993 \pm 2$  d with new RV measurements. Its spectral type was identified to be B9V by Evans (1992c) using the IUE satellite. From HST/GHRS measurements, Bohm-Vitense et al. (1997) measured its orbital velocity amplitude to estimate its mass to be  $3.8 \pm 1.2 M_{\odot}$ . Kervella et al. (2018) derived a similar mass from the analysis of the PM vectors. However, Evans et al. (2005) later obtained HST/STIS spectra of this hot companion and found a large variation in the RV in a short time scale, being  $7 \text{ km s}^{-1}$  change in 4 days. They interpreted this as the companion being itself a short-period binary system, the brighter component being the B9V star.

Such companion would correspond to  $\Delta H \sim 4.9$  mag, which is detectable with the current interferometric recombiner. We observed the Y Car system with VLTI/PIONIER on March 2016 (see Table 1). We have a likely detection at  $6\sigma$  using all observables, while it is not detected at more than  $2.4\sigma$  with the CPs only (see Table 2). Our estimated contrast of  $\sim 5$  mag is in agreement with what expected, however, additional observations will be necessary to firmly conclude about this detection.

We analytically removed this possible companion to estimate the detection limit of a third component, they are listed in Table 3. We can exclude any brighter component with  $\Delta H \lesssim 5.1$  mag.

### 3.5. YZ Car

From RV measurements, Coulson (1983b) discovered that this long-period Cepheid (18.2 d) belongs to a binary system. He derived the preliminary spectroscopic orbital parameters, giving an orbital period of 850 d, and suggested a spectral type between B5V and A5V for this companion. Evans & Butler (1993) later tightened the range of spectral type to B8V-A0V from ultraviolet spectra of the companion. Additional RVs were obtained by Bersier (2002), but he did not revise the orbital elements. A new orbit was fitted by Peterson et al. (2004) combining the

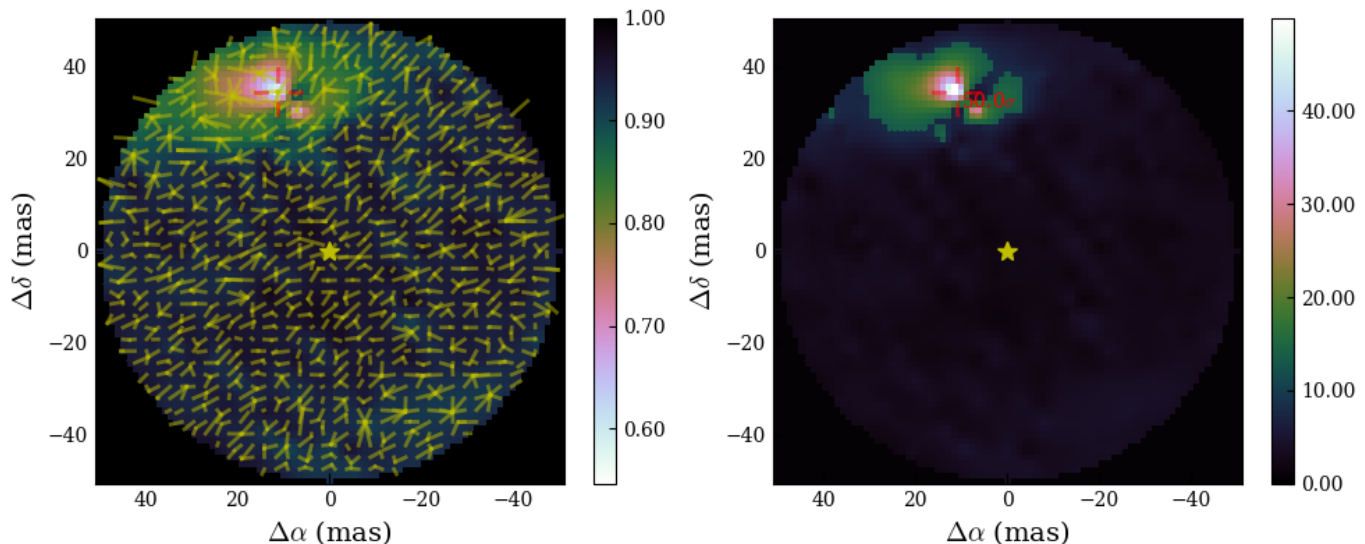


Fig. 3. Same as Fig. 1 but for BP Cir, using all observables.

RVs of Coulson (1983b) with new measurements, and updated the orbital period to 657 d. However, this is not consistent with Coulson’s value, neither with the last determination by Anderson et al. (2016a) who derived  $P_{\text{orb}} = 830$  d, in better agreement with Coulson (1983b). We discuss the possible origin of the disagreement in Sect. 4. Analysis of the PM vectors (Kervella et al. 2018) provides an approximate mass of  $1.9 \pm 0.3 M_{\odot}$ , which is consistent with the expected range of spectral types.

This companion would correspond to a flux ratio in the range 0.1-0.3 %, which is challenging to detect in interferometry. The PIONIER instrument was used on March 2016 and we observed YZ Car two consecutive nights (see Table 1). Unfortunately, the companion is not detected, even combining the two datasets. According to our sensitivity limits (Table 3), we were only able to detect companions with flux ratio  $> 0.75$  % in the best case.

### 3.6. BP Cir

BP Cir is a first overtone Cepheid with a pulsation period of 2.40 days. Its companion was first suggested by Balona (1981) because the Cepheid appeared bluer in his surface brightness-color relation, although he did not detect orbital motion in their RV measurements. Recent and more accurate velocity measurements by Petterson et al. (2004) showed more scatter than expected in the  $\gamma$ -velocity, but it was not sufficient to obtain reliable orbital solutions, suggesting a long orbital period. Such long orbit is consistent with the non-detection in the PM vectors of Kervella et al. (2018).

The blue companion was detected from IUE spectra (Arellano-Ferro & Madore 1985; Evans 1994), and a B6V star best matches the observed spectra. Using the distance  $d = 850$  pc from the  $K$ -band P-L relation for first overtone pulsators (Bono et al. 2002, non-canonical model), we would expect a  $H$ -band flux ratio around 3.2 %.

Our PIONIER observations clearly reveal this companion with a detection level higher than  $50\sigma$  in all observables. The detection maps are presented in Fig. 3, and clearly show the secondary at  $\rho \sim 36.29$  mas with a flux ratio  $f \sim 3.2$ . Our fitted values are reported in Table 2.

The companion was then analytically removed to derive the detection limit for a possible third component. We can exclude

any companion with a flux ratio higher than 1.3 % within 50 mas (see Table 3).

### 3.7. BG Cru

BG Cru is a suspected spectroscopic binary with an orbital period between 4000 and 6650 days (Szabados 1989). Orbital elements are still unknown due to low-precision RVs and a lack of long term measurements. Evans (1992a) did not detect this companion either from IUE spectra, and she set an upper limit on its spectral type to be later than A1V. From PM vector anomaly, Kervella et al. (2018) also flagged this Cepheid as possible binary.

We observed this target with VLTI/PIONIER on 2016 March 4th with the largest available quadruplet. A candidate companion is detected with a moderate detection level. With all observables, we have a detection at  $2.3\sigma$ , while we have  $4.5\sigma$  with only the closure phases. Furthermore, the projected separation and flux ratio are consistent with each other, which add more confidence about this detection. The values are listed in Table 2. This possible detection needs to be confirmed with additional interferometric observations.

The average  $3\sigma$  sensitivity limits are reported in Table 3 (after removing this possible detection). We reached a maximum contrast of 1:130, i.e. a dynamic range of 5.3 mag in the  $H$  band.

### 3.8. T Mon

This long-period Cepheid (27.0 d) has an orbiting hot component discovered by Mariska et al. (1980) from IUE observations, from which they inferred the spectral type to be A0V. The binarity was then confirmed from long-term variations in the RVs (Coulson 1983a; Gieren 1989), but due to the very long orbital period and low-precision RVs, different orbital parameters are found in the literature. Gieren (1989) estimated a period of 175 yr, which is within the range given later by Evans et al. (1999), while the more recent estimate seems to be around  $\sim 89$  yr (Groenewegen 2008). The spectral type of the companion was slightly revised by Evans & Lyons (1994) to be B9.8V. The contrast would correspond to  $\Delta H \sim 8.1$  mag. It is worth mentioning that this

companion is also suspected to be itself a binary (Evans et al. 1999). The small PM anomaly detected by Kervella et al. (2018) confirms the long orbital period.

The PIONIER observations of T Mon are listed in Table 1. We have two observations separated by one month from each other. Neither individual epoch provides significant detection larger than  $2.9\sigma$  (see Table 2). Combining them decrease the detection level to  $2\sigma$  (see Table 3). According to our detection limits, our dataset is sensitive to a contrast  $< 4.9$  mag, and therefore explains that we do not detect this companion.

### 3.9. R Mus

Some evidence that this Cepheid is a spectroscopic binary was given by Lloyd Evans (1982). This was also the conclusion of Szabados (1989) from variations in the systemic velocity. Since then, long term monitoring of the RV of R Mus is still missing, which results in a still unknown orbital period. Evans (1992a) did not detect this companion from IUE spectra, and set an upper limit to A0V for its spectral type. This translates to a flux ratio  $\lesssim 0.35\%$  in the  $H$  band ( $\Delta H \sim 6.1$  mag). From the PM vectors anomaly, Kervella et al. (2018) detected the signature of orbital motion, likely due to this companion.

Our interferometric observations do not reveal this possible companion. We found no significant detection at more than  $1.6\sigma$  (see Table 2). From our derived  $3\sigma$  sensitivity limits, we noticed that this dataset provides a dynamic range of  $\Delta H \sim 5$  mag (see Table 3).

### 3.10. S Mus

This 9.66 d period Cepheid is a known spectroscopic binary. The duplicity was first suspected by Walraven et al. (1964) from multicolor photometry, and Lloyd Evans (1968) from RV measurements. It was later confirmed by Stobie (1970). Several other detections were later reported from IUE spectra and RVs, providing some characteristics of the companion and the spectroscopic orbital solutions (Lloyd Evans 1982; Böhm-Vitense & Proffitt 1985; Bohm-Vitense 1986; Bohm-Vitense et al. 1990; Evans 1990; Petterson et al. 2004). This companion has one of the shortest known orbital period for binary Cepheid systems, which is  $\sim 505$  d.

IUE and HST spectra allowed to estimate the mass ratio by measuring the orbital velocity amplitude of both components (Bohm-Vitense 1986; Evans et al. 1994; Böhm-Vitense et al. 1997). The latest refined value is  $M_{\text{cep}}/M_{\text{comp}} = 1.14$ . The spectral type of the companion was also estimated to be between B3V and B5V, with an average of B3.8V, which would correspond to a  $\sim 5.2 M_{\odot}$  star. This therefore provides an estimate of the Cepheid mass of  $5.9 M_{\odot}$  (Böhm-Vitense et al. 1997). The spectral type was then refined to B3V by Evans et al. (2004) using FUSE spectra, providing a new estimate of the Cepheid mass of  $6.0 M_{\odot}$ . The expected flux ratio in  $H$  for a B3V companion would be  $\sim 1.2\%$ . However, from the PM vectors, Kervella et al. (2018) derived an approximate mass for the companion of  $2.2 M_{\odot}$ , which is not consistent with a B3V star, but with a later spectral type.

We obtained three observing epochs with PIONIER (see Table 1), and the companion is detected for all of them at more than  $5\sigma$ . Our fitted astrometric positions are reported in Table 2. Our measured flux ratio of  $\sim 0.9\%$  is in agreement with the expected value, and would correspond to a slightly later spectral type. A more detailed discussion is presented in Sect. 4.

After removing the companion, we derived the detection limit for a possible third component at each epoch. We can exclude an additional companion with a flux ratio higher than  $0.3\%$  within 50 mas.

### 3.11. S Nor

This Cepheid is possibly a member of a multiple system. One companion has been spatially resolved by Evans et al. (2013) at a separation  $\sim 0.9''$ , with an approximate orbital period of  $\sim 8700$  yrs. Another possible wider and hotter component would be located at  $\sim 36''$ , but the physical association is still uncertain. Orbital motion in RVs is also suspected, maybe linked to another component, but still needs to be confirmed. Szabados (1989) estimated a range of orbital period for this spectroscopic companion between 3300 and 6350 days, but that could not be confirmed by Bersier et al. (1994) who did not find orbital motion larger than  $\sim 0.3 \text{ km s}^{-1}$  from high-precision spectroscopic measurements. Groenewegen (2008) gathered literature data and estimated an orbital period of 3584 days, but fixing the eccentricity to zero. This value is in the range given by Szabados (1989). Using the spectroscopic orbit of Groenewegen (2008) with PM vectors, Kervella et al. (2018) estimated an approximate mass of  $1.5 M_{\odot}$  for a close-in companion, which would correspond to an  $\sim \text{F0V}$  star. From IUE spectra, Evans (1992b) detected a hot companion with a spectral type equivalent to a B9.5V star attributed to one of the wide components. A B9.5V star would correspond to a flux ratio  $f \sim 0.3\%$ , but the wide components are out of the interferometric field of view. If instead this bright companion corresponds to the spectroscopic one, we might be able to detect it from interferometry, otherwise the F0V companion would be more challenging to detect as we would have  $f \sim 0.1\%$ .

We have three epochs of interferometric observations with PIONIER separated by about one year (see Table 1). Unfortunately, we do not have any detection at more than  $2.3\sigma$  (see Table 2). According to our detection limits listed in Table 3, a companion with a flux ratio  $> 0.6\%$  would have been detected at more than  $3\sigma$  from our data. The best detection level is achieved with the CPs by combining the two datasets of 2017, separated by about a month. This is justified by the fact that the orbital period of the spectroscopic component should be between 3300 and 6350 days (Szabados 1989), which would lead to an orbital variation  $< 1\%$ .

### 3.12. W Sgr

This 7.6 d Cepheid is a member of a triple system, composed of a wide and a spectroscopic component. The wide companion was discovered from speckle interferometry by Morgan et al. (1978) at a separation of 116 mas, and later detected at a separation of 160 mas with the HST/STIS by Evans et al. (2009). The same authors identified this wide companion to be the hottest component of the system, previously detected from IUE observations (Böhm-Vitense & Proffitt 1985; Evans 1991). Its spectral type is A0V. The closest companion was discovered by Babel et al. (1989) by combining several RV observations obtained over years and new accurate measurements from the CORAVEL instrument. The first spectroscopic orbital elements have been determined, including an orbital period of 1780 d. The orbit has then been refined with years (Bersier et al. 1994; Petterson et al. 2004; Groenewegen 2008), the latest value being 1651 d. This companion was also detected with the Fine Guidance Sensor (FGS) on board the HST from the orbital reflex motion of the

Cepheid (Benedict et al. 2007). This enabled the determination of the orbital inclination and semi-major axis (12.9 mas). They also provide an estimate for the Cepheid mass of  $6.5 M_{\odot}$  assuming a mass from the companion spectral type. However, Evans et al. (2009) set an upper limit for the spectral type of this companion to be later than F5V, which in turn set an upper limit to the Cepheid mass of  $5.4 M_{\odot}$ . An F5V companion would correspond to a contrast of  $\sim 7.7$  mag ( $f \sim 0.1\%$ ), and will be challenging to detect from interferometry. The approximate mass derived by Kervella et al. (2018,  $0.5 M_{\odot}$ ) is probably too small as it would correspond to an even later spectral type of MOV.

We observed W Sgr with PIONIER as backup target in 2017 (see Table 1). Unfortunately, the companion is not detected from these observations, with a most significant detection level at  $2.7\sigma$  (see Table 2). Our estimated contrast limits shows that with this dataset we were only sensitive to companions brighter than  $f \sim 0.8\%$ .

### 3.13. X Sgr

The binary nature of this system was discovered by Szabados (1990) who gathered RV data from the literature, although Lloyd Evans (1968) already noticed a large scatter in the RVs. Due to the low amplitude of the systemic velocity ( $K \sim 2 - 3 \text{ km s}^{-1}$ ), the spectroscopic orbit determination is difficult, they however estimated an orbital period to be  $\sim 507$  d. This makes the system among the shortest known orbital period binaries containing a Cepheid component in our Galaxy. Evans (1992a) did not detect this companion from IUE spectra, and set an upper limit for the spectral type to be A0V. Two additional RV observations were obtained by Bersier (2002), but insufficient to better constrain the orbit. Since then, no new RV measurements have been published. Groenewegen (2008) recompiled all the RVs from the literature to better constrain the orbital elements, forcing the eccentricity to zero, and derived a period  $P_{\text{orb}} = 573.6$  d. From HST/FGS observations, Benedict et al. (2007) measured the parallax of X Sgr to be  $\pi = 3.00 \pm 0.18$  mas ( $d = 333 \pm 20$  pc), but no detectable perturbation in the Cepheid orbit due to the companion has been noticed. Kervella et al. (2018) detected the signature of a companion from the PM vectors, and estimated an approximate mass for the companion of  $0.5 M_{\odot}$ . Li Causi et al. (2013) argued the detection of the companion at a separation of 10.7 mas with VLTI/AMBER, with a flux ratio of  $f_K \sim 0.6\%$ , but there is no indication about the detection level. Such contrast is difficult to achieve with the current state-of-the-art interferometric recombiner, while AMBER is not designed to reach high-dynamic range. This detection is just at the limit of what this instrument can do, so this detection is uncertain. In addition, their angular diameter estimates are not in agreement with the diameter variation (Breitfelder et al. 2016), where the minimum is around phase 0.8, while they found the opposite at both the minimum and maximum phases. We therefore suspect a spectral calibration problem instead of a binary detection. Furthermore, the expected contrast should be  $\lesssim 0.4\%$  in  $K$  (about the same in  $H$ ), and should be higher at the maximum diameter.

We performed one observation with PIONIER (see Table 1), and such companion should be detectable. We have a detection at  $5.8\sigma$  with the CPs only, while there is no detection using all observables. Although the flux ratio is consistent with what expected (0.4%, see Table 2), it is worth mentioning that two other locations are also possible with similar detection level ( $4.9$  and  $5.2\sigma$ ), so unfortunately we still need confirmation with additional data. Note that these additional locations are spuriously produced by the non-optimal ( $u, v$ ) coverage, as the telescopes

configuration was almost linear (as for V636 Sco, we were also in a non-standard configuration because of strong wind preventing the relocation).

From our estimated  $3\sigma$  detection limit (Table 3), and after removing the possible companion, we can however exclude a companion with a flux ratio larger than 0.7%.

### 3.14. V350 Sgr

This 8.82 d Cepheid has a well known spectroscopic companion. It was confirmed by Gieren (1982) from RV measurements, but was already suspected by Lloyd Evans (1980). Szabados (1990) gave a first estimate of the orbital period (1129 d) by gathering all RVs from the literature for this star. Supplementary RVs over the years enabled the determination of the full spectroscopic orbital element and to refine the period to 1477 d (see e.g. Evans et al. 2011). From IUE observations and spectral template comparison, Evans (1992b) found the spectral type being best matched by a B9V star. This is consistent with the approximate mass of the companion ( $3.4 \pm 0.4 M_{\odot}$ ) derived by Kervella et al. (2018) from the proper motion vectors. Using spectra taken around minimum and maximum orbital phase with the Goddard High Resolution Spectrograph (GHRS) on the HST and assuming a mass for the companion (from a mass-luminosity relation), Evans (2011) estimated a mass for this Cepheid to be  $5.0 \pm 0.7 M_{\odot}$ . This is in agreement with the latest estimate from Peterson et al. (2004) who derived  $6.0 \pm 0.9 M_{\odot}$  with the same method but using new RV measurements. Recently, Evans et al. (2018b) refined the mass to  $5.2 \pm 0.3 M_{\odot}$  using the same method but from new HST/STIS spectra.

According to its spectral type, we should expect a  $H$ -band flux ratio of  $\sim 0.8\%$  for this system. This is detectable with PIONIER. We have three observations with this instrument, which are listed in Table 1. The companion is likely to be detected in the 2013 data, but not in 2017, probably because of the lower quantity of data acquired. The observations of 2013 July 10 have a detection at  $4.5\sigma$  only with all observables, but not with the closure phases only. We also noticed other possible locations with similar detection levels. The observations of 2013 July 14 give a detection with both observables and only the CPs, which is consistent with the detection on 10 July, giving more confidence in this detection. As the orbital change is very small in four days ( $< 0.4\%$ ), we combined the data and fit all the CPs. We found the same location with a detection level of  $\sim 4\sigma$ . This is reported in Table 2. The measured flux ratio of 0.55% is in agreement with expectations, although slightly lower. For the 2017 observations, we do not have a detection at more than  $1.5\sigma$  whatever the observable. This might be due to a lower degree of freedom or the location of the companion too close to the Cepheid to be detected. In any case, additional observations are necessary to fully conclude and have an astrometric orbit.

### 3.15. V636 Sco

The spectroscopic binary nature was first noticed by Feast (1967), but no orbital parameters were derived at that time. The same conclusion was reached by Lloyd Evans (1968) who suggested an orbital period of  $\sim 3.5$  yrs. This was later confirmed by Lloyd Evans (1980), who then followed with the determination of the orbital elements (Lloyd Evans 1982), including an orbital period of 1318 days. Since then, the orbital elements have been updated (see e.g. Böhm-Vitense et al. 1998; Peterson et al. 2004), the latest value being 1362.4 days for the orbital

period. This companion was also detected from IUE spectra by [Böhm-Vitense & Proffitt \(1985\)](#), from which they determined an approximate effective temperature of 9400 K. From additional IUE observations, [Evans \(1992b\)](#) was able to estimate the spectral type for the companion to be B9.5V. [Böhm-Vitense et al. \(1998\)](#) obtained RV measurements around the maximum and minimum orbital velocity using the HST, from which they derived a mass for the Cepheid of  $3.1 M_{\odot}$  (assuming a  $2.5 M_{\odot}$  companion). However, as this is too small for such a 6.8 d pulsating Cepheid, they concluded that the companion might be itself a binary, making the V636 Sco system a probable triple system. Until now, there is no additional evidence to support this. [Kervella et al. \(2018\)](#) derive an approximate mass of  $2.3 M_{\odot}$  for the companion, which is in good agreement with the B9.5V companion (assuming a  $5.1 M_{\odot}$  Cepheid).

A B9.5V companion would give a flux ratio in  $H$  of  $\sim 0.5\%$  ( $\Delta H \sim 6$  mag). To detect this companion, we obtained data from 2013 to 2017 (see Table 1), but we suffered from suboptimal weather conditions. The observations of 2013 do not provide any detection above  $2.3\sigma$  level, probably due to the low quantity of data obtained (see Table 2). In 2015, no signal is detected above  $2.5\sigma$ . The 2016 data suffered from strong seeing variations ( $0.8$ - $1.5''$ ), and do not reveal either this companion. 2017 observations give a detection at a  $3.8\sigma$  level, although we were in a non-standard telescope configuration because of strong wind preventing the relocation. Note that when using all observables, another position gives a similar detection level. So this detection should be considered preliminary.

### 3.16. AH Vel

The binarity of this 4.23 d period Cepheid has been suspected for decades ([Lloyd Evans 1968](#); [Gieren 1977](#); [Lloyd Evans 1982](#); [Szabados 1989](#)) from some variations in the RVs, however the orbital period is still unknown. No obvious trend in the residual of the RVs is seen. [Bersier \(2002\)](#) obtained more precise RV measurements, but only four points which were not enough to confirm the orbit. Since then there has not been additional information about this possible binary system. Recently, [Kervella et al. \(2018\)](#) detected a strong signal in the residuals of the mean proper motion, which is attributed to the close-in companion.

We obtained three observing epochs with PIONIER with about one month interval (see Table 1). We searched for a companion in each epoch individually, but there is no detection at more than  $2.3\sigma$ . These observations were performed in service mode with only a few consecutive observations for the first and third observations (more are needed to detect faint companions), so this non-detection is somewhat expected. The second observation (2017 Jan. 1), which benefited from a longer observing sequence (2 h), does not reveal this companion either. As it is probably on a very long orbital period, we can combine all epoch of closure phase data (not the  $V^2$  as the star has different diameter at each epoch). Unfortunately, there is still no significant detection at more than  $1.2\sigma$ .

We estimate the detection limit from the method explained previously, and are listed in Table 3 for the combined data. We conclude that no companion with a contrast lower than 1:140 is orbiting AH Vel within 50 mas.

## 4. Discussion

In this section we discuss our previous detections and set upper limits for the spectral type of undetected components. We also

**Table 4.** Final estimated parameters of the U Aql system.

		<b>Pulsation</b>	
$P_{\text{puls}}$ (days)		$7.02414 \pm 0.00004$	
$T_0$ (JD) <sup>a</sup>		2 447 755.25	
$A_1$ (km s <sup>-1</sup> )		$-7.47 \pm 0.56$	
$B_1$ (km s <sup>-1</sup> )		$-12.84 \pm 0.35$	
$A_2$ (km s <sup>-1</sup> )		$-7.71 \pm 0.13$	
$B_2$ (km s <sup>-1</sup> )		$-1.36 \pm 0.69$	
$A_3$ (km s <sup>-1</sup> )		$-1.76 \pm 0.35$	
$B_3$ (km s <sup>-1</sup> )		$2.52 \pm 0.22$	
$A_4$ (km s <sup>-1</sup> )		$-0.29 \pm 0.24$	
$B_4$ (km s <sup>-1</sup> )		$1.37 \pm 0.06$	
$A_5$ (km s <sup>-1</sup> )		$0.67 \pm 0.10$	
$B_5$ (km s <sup>-1</sup> )		$0.47 \pm 0.16$	
$A_6$ (km s <sup>-1</sup> )		$0.30 \pm 0.03$	
$B_6$ (km s <sup>-1</sup> )		$-0.02 \pm 0.08$	
		<b>Orbit</b>	
		We87 <sup>b</sup>	This work
$P_{\text{orb}}$ (days)		$1856.4 \pm 4.3$	$1831.4 \pm 6.5$
$T_p$ (JD)		$2\ 442\ 754 \pm 38$	$2\ 457\ 575.3 \pm 8.4$
$e$		$0.165 \pm 0.027$	$0.193 \pm 0.005$
$\omega$ (°)		$190.5 \pm 7.7$	$167.1 \pm 1.9$
$K_1$ (km s <sup>-1</sup> )		$7.81 \pm 0.22$	$8.41 \pm 0.04$
$K_2$ (km s <sup>-1</sup> ) <sup>c</sup>		–	$24.05 \pm 1.24$
$v_{\gamma}$ (km s <sup>-1</sup> )		$1.15 \pm 0.15$	$1.31 \pm 0.06$
$\Omega$ (°)		–	$133.8 \pm 4.4$
$i$ (°)		–	$115.4 \pm 0.7$
$a$ (mas)		–	$10.06 \pm 0.16$
$a$ (au)		–	$5.94 \pm 0.22$
$M_1$ ( $M_{\odot}$ )		–	$6.2 \pm 0.8$
$M_2$ ( $M_{\odot}$ )		–	$2.2 \pm 0.2$
$d$ (pc) <sup>d</sup>		–	$592 \pm 19$

**Notes.**  $P_{\text{orb}}$ : orbital period.  $T_p$ : time passage through periastron.  $e$ : eccentricity.  $K_1, K_2$ : RV semi-amplitude of the primary and secondary.  $v_{\gamma}$ : systemic velocity.  $\omega$ : argument of periastron.  $\Omega$ : position angle of the ascending node.  $a$ : semi-major axis.  $i$ : orbital inclination.  $M_1, M_2$ : mass of primary and secondary.  $P_{\text{puls}}$ : pulsation period.  $T_0$ : reference epoch of maximum light.  $A_i, B_i$ : Fourier parameters.

<sup>(a)</sup> held fixed during the fitting process. <sup>(b)</sup> [Welch et al. \(1987\)](#). <sup>(c)</sup> derived from the orbital elements and the assumed distance. <sup>(d)</sup> assumed from the P-L relation of [Storm et al. \(2011\)](#).

present new high-precision RV measurements, which we used to revise the orbital and pulsation parameters.

**U Aql:** Our three epochs are consistent in terms of flux ratio, i.e. it decreases when the Cepheid diameter increases, making us confident about the detections. The average flux ratio  $0.64 \pm 0.14\%$  (mean and rms of the three values) corresponds to a B8-B9V companion<sup>4</sup>, also in agreement with the IUE observations ([Evans 1992b](#)). We can exclude from our  $3\sigma$  contrast limits (see Table 3) any other companion earlier than a B9V star (after analytically removing the detected one).

Although the listed astrometric positions still need to be confirmed with additional observations, we performed a preliminary orbital fit. As in [Gallenne et al. \(2013\)](#), we combined our astrometry with new high-precision single-line RV data to solve for all the orbital elements. We used new RVs obtained from 2012 to

<sup>4</sup> as previously, interpolated from the grid of [Pecaut & Mamajek \(2013\)](#)

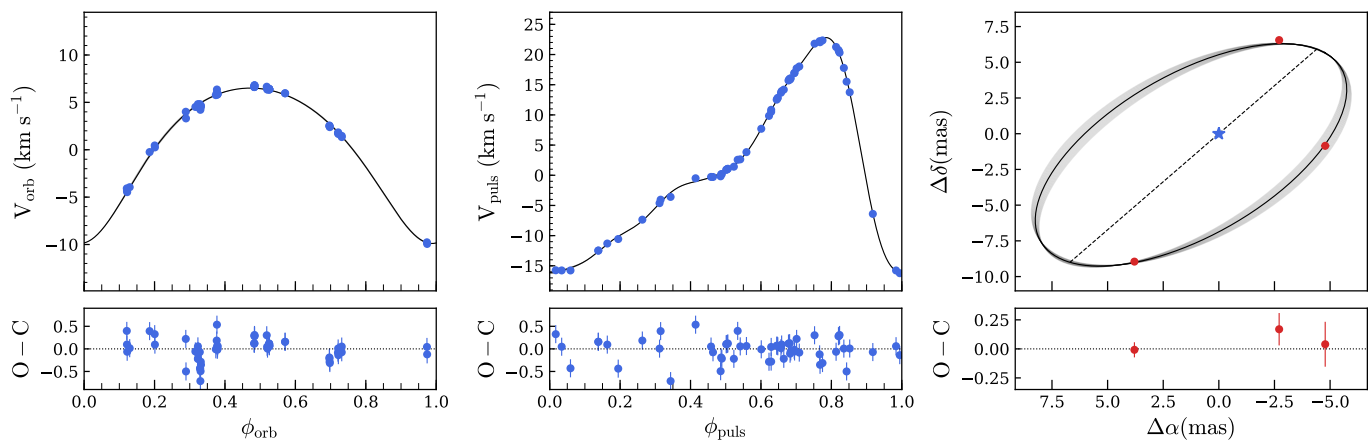


**Fig. 4.** Result of our combined spectroscopic and interferometric fit for U Aql. Left: fitted (solid lines) and measured primary (blue dots) orbital velocity. Middle: fitted (solid line) and measured (blue dots) radial pulsation velocity. Right: relative astrometric orbit of U Aql Ab.

2016 with the SOPHIE, CORALIE and HARPS spectrographs to better constrain the orbit with high-precision data. Data analysis and RV determination are explained in Appendix B, and listed in Table B.1.

The orbital reflex motion of the Cepheid is simultaneously fitted with the radial pulsation using Fourier series of order  $n$  ( $n = 1, 2, \dots$  and depends on the shape of the Cepheid velocity curve). We then followed the formalism detailed in Gallenne et al. (2018a), who used a linear parametrization technique to solve for the orbital and pulsation parameters. The latter is defined with

$$V_{\text{puls}} = \sum_{i=1}^n [A_i \cos(2\pi i \phi_{\text{puls}}) + B_i \sin(2\pi i \phi_{\text{puls}})]. \quad (2)$$

Briefly, we used a Markov chain Monte Carlo (MCMC) fitting routine<sup>5</sup> using the set of nonlinear parameters  $P_{\text{orb}}$ ,  $T_p$  and  $e$  with two other linear parameters (related to  $K_1$ ,  $v_\gamma$  and  $\omega$ ), together with the pulsation parameters ( $P_{\text{puls}}$ ,  $T_0$ , the Fourier parameters  $A_n$ ,  $B_n$ ) and the astrometric Thiele-Innes constants (parametrized in term of the orbital elements  $a$ ,  $\omega$ ,  $\Omega$  and  $i$ ). The names of these variables are defined in Table 4. We adopted as best-fit parameters the median values of the distributions, and used the maximum value between the 16th and 84th percentiles as uncertainty estimates (although the distributions were roughly symmetrical about the median values). Zero point difference was corrected as explained in Appendix B. First guess parameters were taken from Welch et al. (1987, for the orbit, except  $T_p$  where we used our median time value) and Samus et al. (2017, for the pulsation). The final result is plotted in Fig. 4 and the derived parameters are listed in Table 4. The systematic uncertainty from the wavelength calibration of the interferometric data was taken into account and was added quadratically to the error of the semi-major axis. We did not use previous RVs measurements from the literature for several reasons: 1) they are usually not very precise, 2) we wanted a dataset as uniform as possible (i.e. RVs estimated in a homogeneous way), 3) the effect on the RVs of a possible third component is reduced, and 4) we also avoid possible bias from the changing pulsation period of the Cepheid by limiting the time range. Although we find a slightly shorter orbital period, our revised orbital values are in rather good agreement with the previous determination of Welch et al. (1987) from less precise

<sup>5</sup> Using the Python package emcee developed by Foreman-Mackey et al. (2013)

RVs. The systemic velocity is in agreement within  $1\sigma$ , although the value from Welch et al. (1987) has a large uncertainty.

Unfortunately, the distance and masses of both components are degenerate as RVs of the companion are still missing. However, we can have a first estimate of the masses if we assume the distance  $d = 592 \pm 19$  pc from the Cepheid period-luminosity (P-L) relation of Storm et al. (2011). Masses are reported in Table 4, with the uncertainties estimated from the MC simulations including the uncertainty on the distance with a normal distribution centred on 592 pc with a standard deviation of 19 pc. The Gaia parallax from the second data release (GDR2, Gaia Collaboration et al. 2018) was not adopted as its value is very inconsistent with what expected (the value  $1042 \pm 114$  pc is about a factor of two larger than expected). This might be due to the binarity and the changing color and brightness over their pulsation cycle that is not properly taken into account in the GDR2 astrometric pipeline processing.

Our derived mass of the companion is slightly smaller than the one derived by Evans (1992b,  $2.3 M_\odot$ ) from a B9.8V spectral type, but still in agreement within  $1\sigma$ . Our value would be more consistent with an  $\sim A0.5V$  companion. Note however that the distance we used was estimated from an infrared surface-brightness method from the Cepheid photometry, and can be biased by several effects, as for instance the ignored photometric contribution of the companion or the value of the projection-factor. Our preliminary estimate of the Cepheid mass is in agreement with what we expect from evolution models ( $\sim 5.7 M_\odot$ , Evans 2013), although our uncertainty is still large. The mass of  $5.1 \pm 0.7 M_\odot$  inferred by Evans et al. (1998) from measuring the orbital velocity amplitude is also consistent with our estimate.

**FF Aql:** The companion is detected with a low confidence level of  $\sim 2\sigma$ . FF Aql was observed with only one bracket (i.e. one cal-sci-cal sequence), and such high-contrast companion usually needs several hours of observation to be strongly detected. Based on our measured  $H$ -band flux ratio and using the distance  $d = 356$  pc (Benedict et al. 2007), a first estimate of the companion's spectral type would be between B9.5V-F1V. This is consistent with the expected spectral type of the companion A9V-F3V from Evans (1990), although our estimate still depends on the exact Cepheid brightness at that pulsation phase. Note that we assumed main-sequence companions because from an evolution-

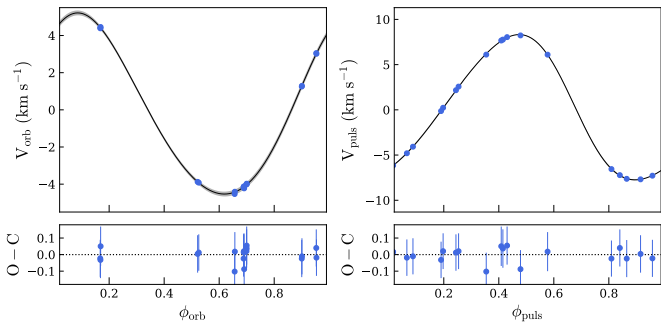


**Fig. 5.** Result of our combined fit of the orbital and radial pulsation velocity for FF Aql. Left: fitted (solid lines) and measured primary (blue dots) orbital velocity. Right: fitted (solid line) and measured (blue dots) radial pulsation velocity.

**Table 5.** Pulsation and orbital parameters of the FF Aql system.

		Pulsation	
$P_{\text{puls}}$ (days)		$4.471036 \pm 0.000015$	
$T_0$ (JD) <sup>a</sup>		2 436 792.539	
$A_1$ (km s <sup>-1</sup> )		$-8.01 \pm 0.10$	
$B_1$ (km s <sup>-1</sup> )		$0.26 \pm 0.88$	
$A_2$ (km s <sup>-1</sup> )		$0.39 \pm 0.21$	
$B_2$ (km s <sup>-1</sup> )		$0.91 \pm 0.11$	
$A_3$ (km s <sup>-1</sup> )		$0.27 \pm 0.04$	
$B_3$ (km s <sup>-1</sup> )		$-0.08 \pm 0.10$	
$A_4$ (km s <sup>-1</sup> )		$-0.02 \pm 0.03$	
$B_4$ (km s <sup>-1</sup> )		$-0.06 \pm 0.02$	
		Orbit	
		Go95 <sup>c</sup>	This work
$P_{\text{orb}}$ (days)		$1433 \pm 5$	$1430.3 \pm 2.6$
$T_p$ (JD)		$2\,445\,381 \pm 10$	$2\,458\,297.0 \pm 13.5$
$e$		$0.09 \pm 0.02$	$0.061 \pm 0.007$
$\omega$ (°)		$327^b$	$316.0 \pm 4.0$
$K_1$ (km s <sup>-1</sup> )		$5 \pm 0.5$	$4.824 \pm 0.008$
$v_\gamma$ (km s <sup>-1</sup> )		$-16 \pm 0.5$	$-16.67 \pm 0.04$
$a_1 \sin i$ (au)		$0.66 \pm 0.07$	$0.633 \pm 0.002$
$f(M)$ ( $M_\odot$ )		$0.018 \pm 0.006$	$0.0166 \pm 0.0001$

**Notes.** Parameters are the same as in Table 4.  $a_1$ : semi-major axis of the Cepheid’s orbit relative to the center of mass.  $f(M)$ : the mass function. <sup>(a)</sup> Not fitted. <sup>(b)</sup> Uncertainty not given by the authors. <sup>(c)</sup> Gorynya et al. (1995).

any time-scale point of view, most of the companions orbiting Cepheids should be stars close to the main sequence.

From our average  $3\sigma$  contrast limits reported in Table 3, we can also exclude any companion orbiting FF Aql within 50 mas with a spectral type earlier than a B9V star. This is compatible with Evans (1992a) who set an upper limit of A1V from an IUE spectrum.

We also revised the spectroscopic orbit using new high-precision RV measurements obtained from 2013 to 2017 with the CORALIE, SOPHIE and HERMES spectrographs. Data analysis and RV determination are explained in Appendix B, and listed in Table B.2. We also used the formalism detailed in Gallenne et al. (2018a), but without the astrometric part. We also did not use previous RV measurements from the literature for the same reasons as explained before. As first guess parameters, we used the values from Gorynya et al. (1995, for the orbit, except  $T_p$  where we used our median time value) and Samus et al.

(2017, for the pulsation).  $T_0$  cannot be properly determined from RVs by definition, so we did not fit this parameter. We corrected for the zero point difference to put the RVs consistent with the CORALIE system, as explained in Appendix B. The final result is plotted in Fig. 5 and the derived parameters are listed in Table 5. The final r.m.s. is small with only  $90 \text{ m s}^{-1}$ . Our revised orbital parameters are in rather good agreement with the literature, within  $1.5\sigma$  (Gorynya et al. 1995; Evans et al. 1990; Abt 1959).

We noticed a slight difference in the systemic velocity between our estimate and the one from Gorynya et al. (1995). This might be linked to the wide companion, however, this might also be due to other non astrophysical effects. We should be cautious when studying long term variations of  $v_\gamma$ , unless a clear pattern is observed. Differences in  $v_\gamma$  of the order of  $0.5\text{--}1 \text{ km s}^{-1}$  might be caused, for instance, to the way RVs are determined (cross-correlation, bisector, ...), the mask used, the instrument zero points, etc... In this paper we did not perform such long term study as this is out of the scope of this paper, and would require a complete analysis of all available literature data.

**U Car:** The companion orbiting this Cepheid is below our detection level. Our datasets enable however to exclude any companion with a flux ratio higher than 0.4 %, which would correspond to a spectral type earlier than B2V (see Table 3).

**Y Car:** Our possibly detected companion has a flux ratio of  $\sim 0.94 \%$ , and would correspond to a  $\sim\text{A0V}$  spectral type, in rather good agreement with the  $\sim\text{B9V}$  derived by Evans (1992c). Although additional data are still necessary to confirm, this possible detection seems in a very close orbit as we measured a projected separation of  $\sim 2.5 \text{ mas}$  ( $\sim 3.5 \text{ au}$ ), as for S Mus.

We first estimated the  $3\sigma$  detection limit using all observables and removing the possible companion (because we have a detection), and second using only the CPs but without removing it (because there is no detection). We noticed that the closure phases alone provide a contrast limit lower than 4 mag (see Table 3), which explains the non-detection with only this observable. With all observables we add more constraints in this case, which provide contrast limit of 5 mag (5.1 mag within 25 mas). This enables us to exclude at  $3\sigma$  any companion with a spectral type earlier than A0V.

**YZ Car:** The faint companion orbiting this Cepheid is not detected from our observations. Our  $3\sigma$  detection limits (see Table 3) show that any companion with a spectral type later than B3V would not have been detected with this dataset, which is consistent with the expected range of spectral type for the companion (B8V–A0V).

New RV data were collected using the HARPS and CORALIE instruments (details in Appendix B, and RVs listed in Table B.3), which span from 2013 to 2015. We used the same formalism as for FF Aql to fit both the pulsation and orbital velocities. The pulsation phase coverage is not optimal to well constrain the pulsation and orbital fits, so we added additional velocities from Anderson et al. (2016a), also obtained with CORALIE from 2014 to 2016. Before combining the data, we compared the systemic velocity of Anderson’s data with ours, and we noticed a positive shift of  $0.8 \text{ km s}^{-1}$ . We therefore corrected for it and simultaneously fitted all dataset. Results are displayed in Fig. 6 and listed in Table 6, with a final r.m.s of  $90 \text{ m s}^{-1}$  ( $190 \text{ m s}^{-1}$  without correcting for the shift). Note that we rescaled the veloc-

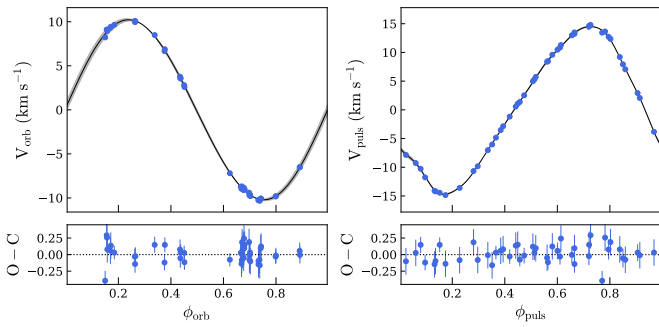


Fig. 6. Same as Fig. 5 but for YZ Car.

Table 6. Final estimated parameters of the YZ Car system.

Pulsation		
$P_{\text{puls}}$ (days)	18.1661 ± 0.0002	
$T_0$ (JD) <sup>a</sup>	2 452 655.37	
$A_1$ (km s <sup>-1</sup> )	-4.57 ± 0.29	
$B_1$ (km s <sup>-1</sup> )	-13.26 ± 0.09	
$A_2$ (km s <sup>-1</sup> )	-0.71 ± 0.03	
$B_2$ (km s <sup>-1</sup> )	-0.81 ± 0.02	
$A_3$ (km s <sup>-1</sup> )	-0.02 ± 0.04	
$B_3$ (km s <sup>-1</sup> )	0.65 ± 0.01	
$A_4$ (km s <sup>-1</sup> )	-0.06 ± 0.04	
$B_4$ (km s <sup>-1</sup> )	0.36 ± 0.01	
$A_5$ (km s <sup>-1</sup> )	-0.15 ± 0.01	
$B_5$ (km s <sup>-1</sup> )	0.01 ± 0.02	
$A_6$ (km s <sup>-1</sup> )	-0.24 ± 0.01	
$B_6$ (km s <sup>-1</sup> )	-0.07 ± 0.03	
$A_7$ (km s <sup>-1</sup> )	-0.17 ± 0.01	
$B_7$ (km s <sup>-1</sup> )	-0.06 ± 0.03	
$A_8$ (km s <sup>-1</sup> )	-0.12 ± 0.01	
$B_8$ (km s <sup>-1</sup> )	-0.01 ± 0.02	
Orbit		
	An16 <sup>b</sup>	This work
$P_{\text{orb}}$ (days)	830.22 ± 0.34	831.6 ± 0.9
$T_p$ (JD)	2 453 422 ± 29	2 453 565.8 ± 13.7
$e$	0.041 ± 0.010	0.035 ± 0.003
$\omega$ (°)	195 ± 12	260.5 ± 6.8
$K_1$ (km s <sup>-1</sup> )	10.26 ± 0.82	10.249 ± 0.019
$v_\gamma$ (km s <sup>-1</sup> )	0.84 ± 0.06	0.02 ± 0.03
$a_1 \sin i$ (au)	0.783 ± 0.063	0.783 ± 0.002
$f(M)$ ( $M_\odot$ )	0.093 ± 0.041	0.0926 ± 0.0005

Notes. <sup>(a)</sup> Not fitted. <sup>(b)</sup> Anderson et al. (2016a).

ity uncertainties of Anderson’s data to 0.19 km s<sup>-1</sup> (r.m.s. of the residual without rescaling) to compensate for the use of a different binary mask in the RV determination. Our revised orbital solutions are in good agreement with Anderson et al. (2016a). We therefore confirm the orbital period of ~ 830 d, in disagreement with the 657 d estimated by Petterson et al. (2004), as also noted by Anderson et al. (2016a). As mentioned previously, Petterson et al. (2004) used different dataset spanning several decades which can lead to biases if, for instance, period change is not taken into account.

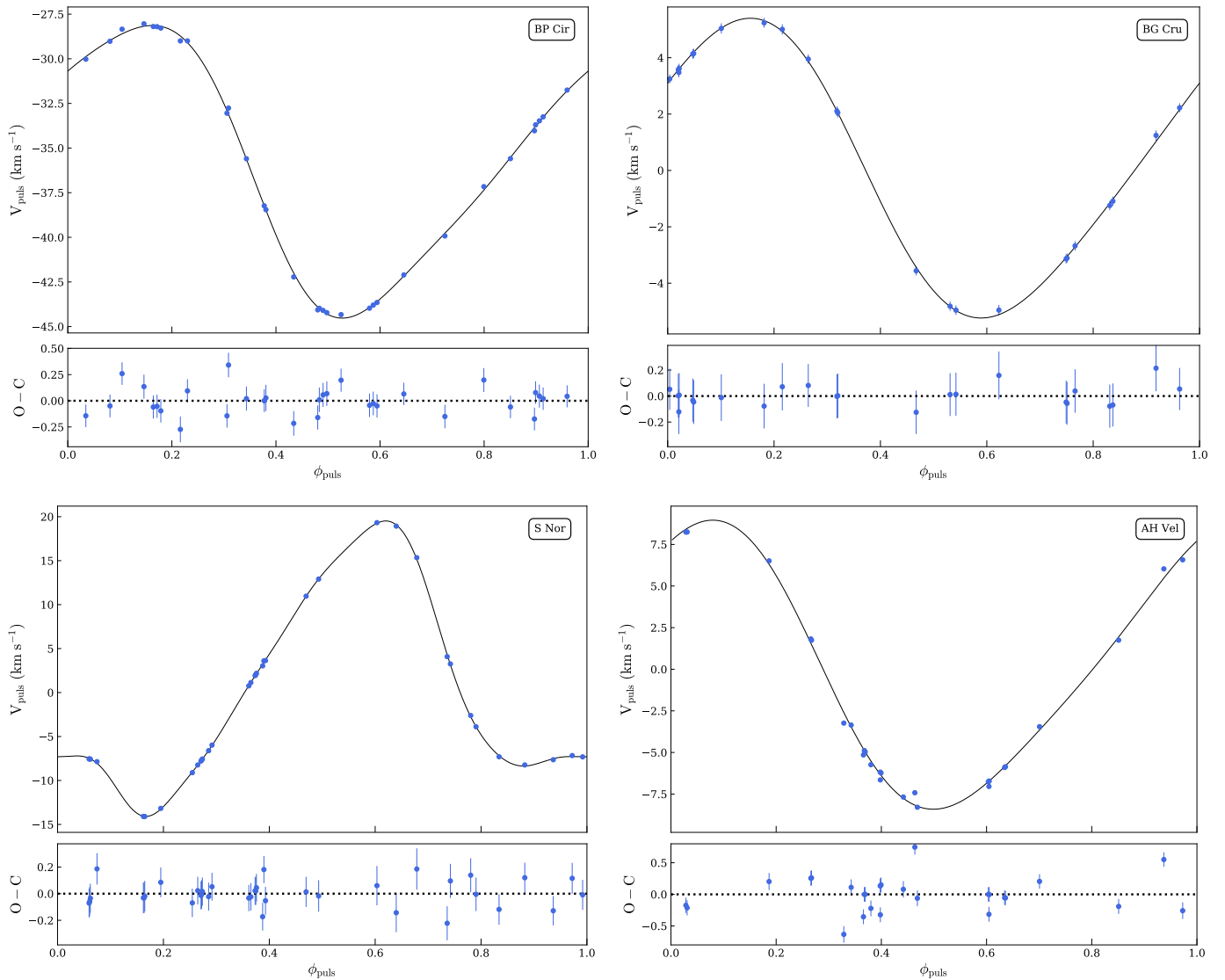
BP Cir: We confirm the presence of a companion orbiting the Cepheid. Our measured flux ratio is in very good agreement with

Table 7. Final estimated pulsation parameters of BP Cir, BG Cru, S Nor and AH Vel.

BP Cir		
	Pe04 <sup>c</sup>	This work
$P_{\text{puls}}$ (days)	2.39819 ± 0.00005	2.398131 ± 0.000001
$T_0$ (JD)	2 444 297.03	2 456 828.21 ± 0.03
$A_1$ (km s <sup>-1</sup> )	–	-0.45 ± 0.59
$B_1$ (km s <sup>-1</sup> )	–	7.80 ± 0.05
$A_2$ (km s <sup>-1</sup> )	–	0.47 ± 0.23
$B_2$ (km s <sup>-1</sup> )	–	-1.54 ± 0.09
$A_3$ (km s <sup>-1</sup> )	–	-0.26 ± 0.074
$B_3$ (km s <sup>-1</sup> )	–	0.33 ± 0.07
$v_\gamma$ (km s <sup>-1</sup> )	19.0	18.00 ± 0.11
BG Cru		
	Sz89	This work
$P_{\text{puls}}$ (days)	3.34272 ± 0.00001	3.342536 ± 0.000003
$T_0$ (JD)	2 440 393.660 ± 0.08	2 456 753.93 ± 0.09
$A_1$ (km s <sup>-1</sup> )	–	3.48 ± 0.68
$B_1$ (km s <sup>-1</sup> )	–	3.86 ± 0.52
$A_2$ (km s <sup>-1</sup> )	–	-0.58 ± 0.03
$B_2$ (km s <sup>-1</sup> )	–	0.02 ± 0.19
$v_\gamma$ (km s <sup>-1</sup> )	-19.6 ± 0.3 <sup>a</sup>	-20.00 ± 0.18
S Nor		
	Me87 <sup>d</sup>	This work
$P_{\text{puls}}$ (days)	9.7544 ± 0.0005	9.75473 ± 0.00001
$T_0$ (JD)	2 445 397.507	2 444 018.13 ± 0.05
$A_1$ (km s <sup>-1</sup> )	–	-12.25 ± 0.20
$B_1$ (km s <sup>-1</sup> )	–	-6.85 ± 0.37
$A_2$ (km s <sup>-1</sup> )	–	3.39 ± 0.20
$B_2$ (km s <sup>-1</sup> )	–	3.53 ± 0.22
$A_3$ (km s <sup>-1</sup> )	–	2.57 ± 0.03
$B_3$ (km s <sup>-1</sup> )	–	-0.24 ± 0.23
$A_4$ (km s <sup>-1</sup> )	–	-0.33 ± 0.01
$B_4$ (km s <sup>-1</sup> )	–	-0.10 ± 0.04
$A_5$ (km s <sup>-1</sup> )	–	-0.36 ± 0.09
$B_5$ (km s <sup>-1</sup> )	–	0.58 ± 0.05
$A_6$ (km s <sup>-1</sup> )	–	-0.05 ± 0.01
$B_6$ (km s <sup>-1</sup> )	–	-0.01 ± 0.01
$A_7$ (km s <sup>-1</sup> )	–	-0.24 ± 0.03
$B_7$ (km s <sup>-1</sup> )	–	-0.17 ± 0.05
$A_8$ (km s <sup>-1</sup> )	–	-0.04 ± 0.02
$B_8$ (km s <sup>-1</sup> )	–	-0.09 ± 0.01
$v_\gamma$ (km s <sup>-1</sup> )	5.85 ± 0.06	5.14 ± 0.12
AH Vel		
	Sz89 <sup>b</sup>	This work
$P_{\text{puls}}$ (days)	4.227231 ± 0.000007	4.227527 ± 0.000001
$T_0$ (JD)	2 442 035.703 ± 0.07	2 456 605.05 ± 0.08
$A_1$ (km s <sup>-1</sup> )	–	7.99 ± 0.36
$B_1$ (km s <sup>-1</sup> )	–	2.50 ± 0.93
$A_2$ (km s <sup>-1</sup> )	–	-0.42 ± 0.26
$B_2$ (km s <sup>-1</sup> )	–	1.15 ± 0.13
$v_\gamma$ (km s <sup>-1</sup> )	24.5 ± 0.3 <sup>a</sup>	24.68 ± 0.13

Notes. <sup>(a)</sup> From Gieren (1977) for AH Vel, from Stobie & Balona (1979a) for BG Cru. <sup>(b)</sup> Szabados (1989). <sup>(c)</sup> Petterson et al. (2004). <sup>(d)</sup> Mermilliod et al. (1987).

the detection from IUE spectra (Evans 1994) for a B6V star. From our measured projected separation,  $\rho$ , and the Kepler’s third law, we can estimate a lower limit for the orbital period as we know that the semi-major axis  $a > \rho$ . Adopting a mass



**Fig. 7.** Fitted radial pulsation velocity curve of BP Cir, BG Cru, S Nor and AH Vel.

$M_2 = 4.7 M_\odot$  for the companion,  $M_1 = 4.9 M_\odot$  for the Cepheid (Evans et al. 2013), the distance  $d = 850$  pc and 15 % uncertainty on those values, we found  $P_{\text{orb}} \gtrsim 40$  years.

There is no existing infrared light curve for BP Cir to estimate its magnitude at our given pulsation phase. We therefore took the value  $m_H = 5.58 \pm 0.04$  mag given by Cutri et al. (2MASS catalog 2003). To take into account the phase mismatch with the mean magnitude, we also quadratically added a conservative uncertainty of 0.06 mag, which corresponds to half the amplitude of the light curve in the  $I$  band (Berdnikov 2008, probably smaller in  $H$ ). We estimated the magnitudes  $m_H(\text{comp}) = 9.35 \pm 0.10$  mag and  $m_H(\text{cep}) = 5.61 \pm 0.07$  mag.

According to our estimated detection limits listed in Table 3, we did not detect additional companions within 50 mas with a flux ratio larger than 1.3 %, corresponding to an upper limit of approximately A2V for the spectral type (assuming  $d = 850$  pc).

Spectra for this Cepheid were also obtained with the HARPS and SOPHIE spectrographs from 2013 to 2015 (see Table B.4). Differently to our previous analysis, for which we had first guesses of the orbital parameters, we first analysed our RVs by fitting only the pulsation of the Cepheid with Fourier series as described in Eq. (2), in which we added the systemic velocity

$v_\gamma$ . The curve is displayed in Fig. 7, and the fitted parameters are listed in Table 7. Here, we performed a simple Monte Carlo simulation by randomly creating 1 000 synthetic RVs around our best fit solutions. We used normal distributions with standard deviations corresponding to the measurement uncertainties. We then took the median value of the distributions and used the maximum value between the 16th and 84th percentiles as uncertainty estimates. We used only  $n = 3$  Fourier coefficients as the fit is not improved by using an order 4. The residuals are very small with a r.m.s of  $0.14 \text{ km s}^{-1}$ . This confirms a very long orbital period, which is also consistent with the location of our detected component. To search for a sign of modulation, we generated a Lomb-Scargle periodogram<sup>6</sup> including older RV measurements (Balona 1981; Petterson et al. 2004, 2005, and ignoring a possible period change). We restricted our period search to twice the longest time span of the data (i.e.  $P_{\text{max}} = 2(t_{\text{max}} - t_{\text{min}})$ , to cover at least half an orbital period), while the minimum period is set to 400 days (about the shortest possible orbital period for Cepheids in binary systems, according to Neilson et al. 2015). We found

<sup>6</sup> We used the *astroML* python module and its bootstrapping package to find the significance levels (VanderPlas et al. 2012)

several peaks with a high probability (false alarm probability  $FAP < 0.1\%$ ), the strongest being at a period of  $\sim 14680$  days, then 6790 and 4500 days. The two last values are too small to be consistent with our measured astrometric position, but the first one is in agreement with the lower limit estimated above. We stress that such analysis assumes a zero eccentricity and ignores pulsation period change. We unfortunately cannot yet determine the orbital period only from spectroscopy, but additional astrometric measurements will better constrain the orbit in a few years.

**BG Cru:** The expected companion should have a spectral type later than a A1V star according to the detection limit set by [Evans \(1992a\)](#). This means that the flux ratio should be  $\lesssim 0.5\%$ . Our measured flux ratio for this possible detection is  $0.53 \pm 0.12\%$ , in agreement with this detection limit, and corresponds to a companion with a spectral type in the range B9V-A4V.

From our detection limits, we reached the same conclusion as [Evans \(1992a\)](#) within 50 mas from the Cepheid, i.e. there is no companion with a spectral type earlier than A2V.

We performed the same analysis as for BP Cir with new high-precision RV data (see Appendix B). The pulsation curve is displayed in Fig. 7 and the fitted parameters in Table 7. The residuals are small ( $0.8 \text{ km s}^{-1}$ ), suggesting no spectroscopic companion, a very long orbital period or a high orbital inclination. The periodogram for these data do not show sign of any significant peak ( $FAP = 9.1\%$ ). We included older (less precise) RVs collected from the literature ([Lloyd Evans 1980](#); [Stobie & Balona 1979b](#); [Usenko et al. 2014](#)) and calculated the periodogram. There is a significant peak (with a  $FAP < 0.1\%$ ) at a period of  $\sim 5365$  days. This period would be consistent with [Szabados \(1989\)](#) who found a  $\sim 5000$  day pattern from the light time effect. However we cannot exclude other peaks with similar significant levels (with  $FAP < 1\%$ ). Additional high-precision RVs will be necessary to confirm this period.

**T Mon:** The spectroscopic companion is also below our sensitivity limit. Our estimated detection level is  $\Delta H \sim 4.7$  mag, well below the 8.1 mag required to detect it. However, although a brighter component is unlikely, we can still rule out an orbiting companion brighter than  $H \sim 7.4$  mag, which would correspond to a companion earlier than a B1V star (see Table 3).

**R Mus:** We cannot confirm from our interferometric observations the presence of the spectroscopic companion. Its expected flux ratio is  $f_H \lesssim 0.4\%$ , while our detection limits show that with this dataset we were sensitive to the companion having  $f_H > 1\%$ . We can however reject the presence of any companion brighter than a B8V star within 50 mas.

**S Mus:** We confirm the presence of a close-in companion. The contrast is slightly higher than the expected value, a  $\sim$  B6V being more appropriate, but detections in more photometric bands are necessary to better constrain the spectral type. Our estimated detection limits enable us to exclude any possible third component with a spectral type earlier than B9V.

As for U Aql, we performed a preliminary MCMC orbital fit by combining our astrometry with single-line RVs to solve for all the orbital elements. The resulting parameters are listed in Table 8 and plotted in Fig 8. We remove the degeneracy between the mass and the distance using a P-L relation ([Storm et al.](#)

**Table 8.** Final estimated parameters of the S Mus system.

Pulsation		
$P_{\text{puls}}$ (days)	$9.65996 \pm 0.00006$	
$T_0$ (JD) <sup>a</sup>	2 440 299.42	
$A_1$ (km s <sup>-1</sup> )	$-6.94 \pm 0.82$	
$B_1$ (km s <sup>-1</sup> )	$-9.81 \pm 0.54$	
$A_2$ (km s <sup>-1</sup> )	$-4.53 \pm 0.67$	
$B_2$ (km s <sup>-1</sup> )	$3.87 \pm 0.79$	
$A_3$ (km s <sup>-1</sup> )	$-0.60 \pm 0.34$	
$B_3$ (km s <sup>-1</sup> )	$1.46 \pm 0.15$	
$A_4$ (km s <sup>-1</sup> )	$0.86 \pm 0.10$	
$B_4$ (km s <sup>-1</sup> )	$0.23 \pm 0.24$	
$A_5$ (km s <sup>-1</sup> )	$0.21 \pm 0.04$	
$B_5$ (km s <sup>-1</sup> )	$-0.05 \pm 0.10$	
Orbit		
	Pe04 <sup>b</sup>	This work
$P_{\text{orb}}$ (days)	$504.9 \pm 0.07$	$506.3 \pm 0.5$
$T_p$ (JD)	$2\,448\,590 \pm 5$	$2\,457\,165.9 \pm 4.4$
$e$	$0.080 \pm 0.002$	$0.088 \pm 0.006$
$\omega$ (°)	$206 \pm 5$	$194.8 \pm 3.3$
$K_1$ (km s <sup>-1</sup> )	$14.7 \pm 0.2$	$14.85 \pm 0.03$
$K_2$ (km s <sup>-1</sup> ) <sup>c</sup>	–	$16.63 \pm 3.27$
$v_\gamma$ (km s <sup>-1</sup> )	$-0.5 \pm 0.5$	$-1.65 \pm 0.11$
$\Omega$ (°)	–	$99.6 \pm 14.4$
$i$ (°)	–	$144.7 \pm 2.8$
$a$ (mas)	–	$2.95 \pm 0.09$
$a$ (au)	–	$2.53 \pm 0.09$
$M_1$ ( $M_\odot$ )	–	$4.44 \pm 0.91$
$M_2$ ( $M_\odot$ )	–	$3.98 \pm 0.21$
$d$ (pc) <sup>d</sup>	–	$858 \pm 17$

**Notes.** <sup>(a)</sup> held fixed with the value from [Samus et al. \(2017\)](#). <sup>(b)</sup> [Pettersson et al. \(2004\)](#). <sup>(c)</sup> derived from the orbital elements and the assumed distance. <sup>(d)</sup> assumed from the P-L relation of [Storm et al. \(2011\)](#).

2011), giving  $d = 858 \pm 17$  pc. First guess values were taken from [Pettersson et al. \(2004\)](#) and [Samus et al. \(2017\)](#).

Our estimated mass ratio is in agreement with the 0.88 derived by [Böhm-Vitense et al. \(1997\)](#). The Cepheid mass is in slight agreement with the  $6.0 \pm 0.4 M_\odot$  estimate by [Evans et al. \(2004\)](#) from the FUSE spectra, but this is expected as they used  $q = 0.88$ . Our derived companion mass is also smaller than the one for a B3V star ( $\sim 5.3 M_\odot$ ), and would be more compatible with a B6V star, which is also consistent with our measured flux ratio. However, this is still preliminary and the astrometric orbit will have a better coverage soon.

Finally, let us also note that from our average  $3\sigma$  contrast limits (see Table 3), we exclude any additional companion within 50 mas from the Cepheid with a spectral type earlier than B9V.

**S Nor:** The possible spectroscopic component is expected to have a contrast  $\sim 0.3\%$  ( $\Delta H \sim 6.4$  mag), but this is just below the sensitivity limit of our datasets (see Table 3), which is consistent with our non-detection. We are therefore not able to confirm the presence of a close-in companion. From our detection limit, we can exclude a companion brighter than  $H = 5.6$  mag within 25 mas, and brighter than 5.3 mag within 25-50 mas, which correspond to stars with spectral type earlier than B7V and B5V, respectively.

New RVs were also collected for this Cepheid from 2013 to 2018 using both the CORALIE and HARPS spectrographs (see

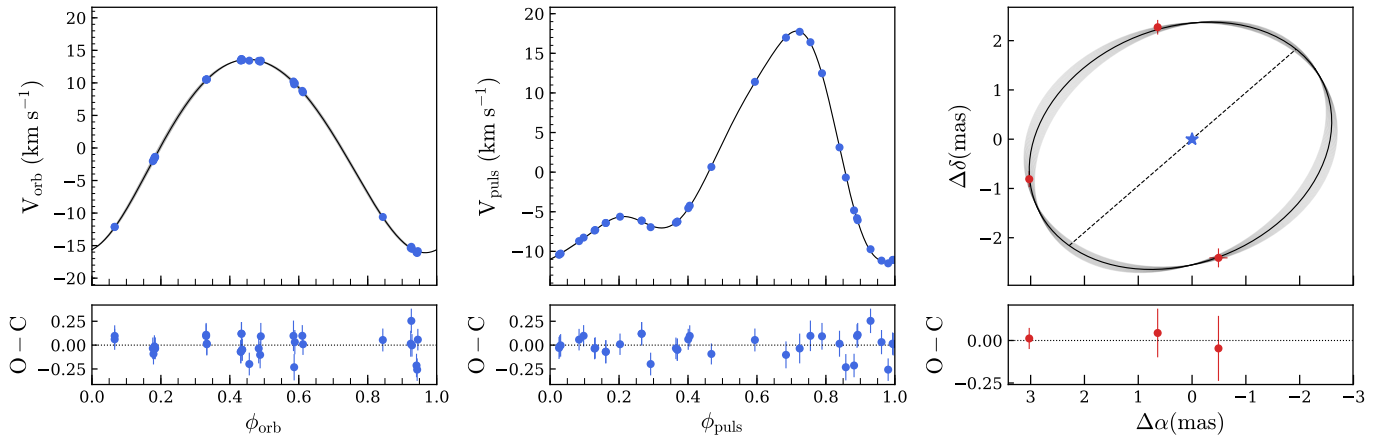


**Fig. 8.** Result of our combined fit for S Mus. Left: fitted (solid lines) and measured primary (blue dots) orbital velocity. Middle: fitted (solid line) and measured (blue dots) radial pulsation velocity. Right: relative astrometric orbit of S Mus Ab.

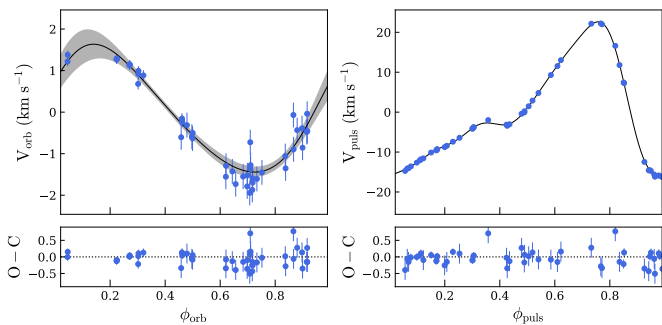


**Fig. 9.** Same as Fig. 5 but for W Sgr.

Appendix B for details). RVs are listed in Table B.7. These observations span half the period of  $\sim 10$  yrs given by Groenewegen (2008), so the orbital motion should be detected from our new observations. As previously, we first fitted the pulsation of the star. The parameters and the pulsation curve are in Table 7 and Fig. 7, respectively. The r.m.s of the fit is  $90 \text{ m s}^{-1}$ . After correcting for the pulsation, the residual periodogram does not show any significant peak, the highest being at a too short period of 760 d with a FAP = 3%. We increased the time span by including RVs from Bersier et al. (1994, with a zero point correction as given by Udry et al. 1999), but there is also no significant peak in the residual periodogram, the highest being at 836 d with a FAP = 14%. We suggest that S Nor is probably not a spectroscopic binary. The other possibility would be that this hypothetical companion has a very low mass, and might have a high orbital inclination.

**W Sgr:** The spectroscopic component is not detected from our interferometric observations. We estimated the  $3\sigma$  detection level to be  $\Delta H = 5.1 \text{ mag}$  (see Table 3), which is not enough to detect the F5V companion ( $\Delta H \sim 7.7 \text{ mag}$ ). However, this limit enables us to rule out any component with a spectral type earlier than B8V.

New RVs were collected for W Sgr from the HARPS, CORALIE and HERMES instruments (details in Appendix B and RVs are given in Table B.8), spanning from 2013 to 2017. We did not use RVs measurements from the literature as explained previously. The combined fit is displayed in Fig. 9, and

**Table 9.** Final estimated parameters of the W Sgr system.

Pulsation		
$P_{\text{puls}}$ (days)	7.59508 + / - 0.00002	
$T_0$ (JD) <sup>a</sup>	2 443 374.77	
$A_1$ (km s <sup>-1</sup> )	$-9.86 \pm 0.33$	
$B_1$ (km s <sup>-1</sup> )	$-10.70 \pm 0.31$	
$A_2$ (km s <sup>-1</sup> )	$-7.47 \pm 0.23$	
$B_2$ (km s <sup>-1</sup> )	$3.38 \pm 0.46$	
$A_3$ (km s <sup>-1</sup> )	$0.31 \pm 0.24$	
$B_3$ (km s <sup>-1</sup> )	$2.59 \pm 0.04$	
$A_4$ (km s <sup>-1</sup> )	$1.12 \pm 0.17$	
$B_4$ (km s <sup>-1</sup> )	$1.30 \pm 0.15$	
$A_5$ (km s <sup>-1</sup> )	$0.40 \pm 0.09$	
$B_5$ (km s <sup>-1</sup> )	$-0.57 \pm 0.06$	
$A_6$ (km s <sup>-1</sup> )	$0.17 \pm 0.08$	
$B_6$ (km s <sup>-1</sup> )	$-0.43 \pm 0.04$	
$A_7$ (km s <sup>-1</sup> )	$0.03 \pm 0.01$	
$B_7$ (km s <sup>-1</sup> )	$-0.21 \pm 0.04$	
$A_8$ (km s <sup>-1</sup> )	$-0.05 \pm 0.02$	
$B_8$ (km s <sup>-1</sup> )	$0.06 \pm 0.01$	
$A_9$ (km s <sup>-1</sup> )	$0.12 \pm 0.02$	
$B_9$ (km s <sup>-1</sup> )	$0.06 \pm 0.03$	
$A_{10}$ (km s <sup>-1</sup> )	$0.06 \pm 0.01$	
$B_{10}$ (km s <sup>-1</sup> )	$-0.04 \pm 0.01$	
Orbit		
$P_{\text{orb}}$ (days)	Pe04 <sup>b</sup>	This work
$T_p$ (JD)	$1582 \pm 9$	$1615.5 \pm 11.0$
$e$	$2\,448\,286$	$2\,457\,992.4 \pm 19.5$
$\omega$ (°)	$0.41 \pm 0.05$	$0.197 \pm 0.018$
$K_1$ (km s <sup>-1</sup> )	$328 \pm 5$	$288.4 \pm 5.7$
$v_y$ (km s <sup>-1</sup> )	$1.08 \pm 0.03$	$1.562 \pm 0.011$
$a_1 \sin i$ (au)	$-26.0 \pm 0.1$	$-27.87 \pm 0.02$
$f(M)$ ( $M_{\odot}$ )	$0.143$	$0.228 \pm 0.003$
	$0.157 (\times 10^3)$	$0.60 \pm 0.02 (\times 10^3)$

**Notes.** <sup>(a)</sup> Not fitted. <sup>(b)</sup> Petterson et al. (2004).

the revised orbit in Table 9. The same fitting formalism as for FF Aql was applied. The residual standard deviation is  $80 \text{ m s}^{-1}$ . Our newly derived orbit is in slight agreement with previous de-

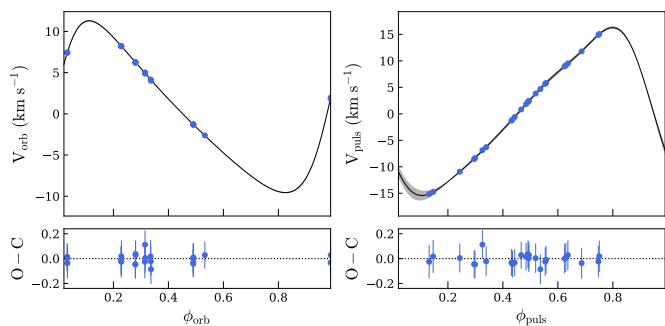


**Fig. 10.** Same as Fig. 5 but for V350 Sgr.

terminations (Babel et al. 1989; Bersier et al. 1994; Albrow & Cottrell 1996). However, such low-amplitude orbit is difficult to constrain as it needs continuous high-precision measurements to allow a good determination of the orbit. Combining several datasets is usually not optimal as several additional effects can alter the results, as for instance the presence of a third component, the pulsation period change, or the method used to estimate the RVs. To well constrain such low amplitude binary, this is critical to control such effects.

X Sgr: The spectroscopic component is possibly detected at a separation of  $\sim 14$  mas with the closure phase signal only, but additional observations are necessary to firmly conclude. Our measured flux ratio is compatible with a B9-A2V star, in agreement with the limit set by Evans (1992a). From our estimated detection limit (Table 3), we are also able to exclude any additional component with a contrast lower than  $\sim 1 : 140$ , which would correspond to companions with a spectral type earlier than B8V.

V350 Sgr: Our candidate companion has an  $H$ -band flux ratio of  $0.55 \pm 0.11\%$  which corresponds to approximately a B9V-A1V star. This is in agreement with the B9V spectral type estimated by Evans (1992b, see also Evans et al. 2018b). Additional astrometric data are still necessary to confirm.

The  $3\sigma$  detection limits of the 2013 and 2017 observations are listed in Table 3. The 2017 observations give a B8V limit, which is consistent with our non-detection. The 2013 data give, after removing the detected component, a detection level  $\Delta H = 5.3$  mag, and enable us to exclude additional companions earlier than B8V.

A new set of RVs has been obtained with the CORALIE and HARPS spectrographs (details in Appendix B), collected from 2013 to 2015. Due to our limited dataset which has a poor orbital and pulsation phase coverage, we also collected RVs from Evans et al. (2011). By fitting the two datasets separately, we noticed a systemic velocity difference of  $1.45 \text{ km s}^{-1}$ , which we subtracted from Evans' data. We took as first guess values for the orbit and pulsation the ones derived by Evans et al. (2011), and applied the same fitting formalism as for FF Aql. In Fig. 10 are displayed the pulsation and orbital velocity curves, and our revised parameters in Table 10. Our values are in slight agreement with previous works (Evans et al. 2011; Petterson et al. 2004), with a final r.m.s. of the residual of  $330 \text{ m s}^{-1}$ . However, here we only collected the data provided by Evans (taken from 2005 by Eaton) and we did not combine with additional data from the literature.

**Table 10.** Final estimated parameters of the V350 Sgr system.

			<b>Pulsation</b>	
$P_{\text{puls}}$ (days)			$5.154151 \pm 0.000008$	
$T_0$ (JD) <sup>a</sup>			$2\ 440\ 146.6156$	
$A_1$ ( $\text{km s}^{-1}$ )			$-5.37 \pm 0.42$	
$B_1$ ( $\text{km s}^{-1}$ )			$-14.00 \pm 0.17$	
$A_2$ ( $\text{km s}^{-1}$ )			$-3.76 \pm 0.25$	
$B_2$ ( $\text{km s}^{-1}$ )			$-4.22 \pm 0.23$	
$A_3$ ( $\text{km s}^{-1}$ )			$-2.72 \pm 0.10$	
$B_3$ ( $\text{km s}^{-1}$ )			$-0.97 \pm 0.25$	
$A_4$ ( $\text{km s}^{-1}$ )			$-1.26 \pm 0.02$	
$B_4$ ( $\text{km s}^{-1}$ )			$0.20 \pm 0.14$	
$A_5$ ( $\text{km s}^{-1}$ )			$-0.39 \pm 0.06$	
$B_5$ ( $\text{km s}^{-1}$ )			$0.42 \pm 0.07$	
$A_6$ ( $\text{km s}^{-1}$ )			$-0.05 \pm 0.05$	
$B_6$ ( $\text{km s}^{-1}$ )			$0.29 \pm 0.01$	
$A_7$ ( $\text{km s}^{-1}$ )			$0.11 \pm 0.03$	
$B_7$ ( $\text{km s}^{-1}$ )			$0.14 \pm 0.02$	
			<b>Orbit</b>	
$P_{\text{orb}}$ (days)			Ev11 <sup>b</sup>	This work
$T_p$ (JD)			$1472.91 \pm 1.33$	$1465.3 \pm 0.4$
$e$			$2\ 450\ 526.63 \pm 6.60$	$2\ 450\ 554.6 \pm 2.2$
$\omega$ ( $^\circ$ )			$0.369 \pm 0.011$	$0.336 \pm 0.003$
$K_1$ ( $\text{km s}^{-1}$ )			$279.03 \pm 1.72$	$283.7 \pm 0.7$
$v_\gamma$ ( $\text{km s}^{-1}$ )			$10.59 \pm 0.10$	$10.38 \pm 0.03$
$a_1 \sin i$ (au)			$11.36 \pm 0.07$	$10.11 \pm 0.02$
$f(M)$ ( $M_\odot$ )			$1.330 \pm 0.014$	$1.317 \pm 0.004$
			$0.146 \pm 0.005$	$0.142 \pm 0.001$

**Notes.** <sup>(a)</sup> not fitted. <sup>(b)</sup> Evans et al. (2011).

V636 Sco: Despite several epoch observations, we did not succeed in detecting the companion. Such faint companions (i.e.  $f \lesssim 0.5\%$ ) are difficult to detect and need optimal observing conditions. Table 3 lists the  $3\sigma$  detection limits for our observations. Within 50 mas, we can rule out a companion with a contrast lower than  $\Delta H = 5.8$  mag (i.e. with a flux ratio  $> 0.5\%$ ), which would correspond to spectral types earlier than B9V.

New RVs have been obtained with the CORALIE and HARPS spectrographs (details in Appendix B, and RVs are given in Table B.10), spanning from 2013 to 2015. As our dataset is limited and did not have a sufficient phase coverage, we combined them with RVs from Petterson et al. (2004). We noticed that their zero point is shifted by  $1 \text{ km s}^{-1}$ , which we corrected for our combined fit. We took as first guess values to fit the pulsation and orbit the ones derived by Böhm-Vitense et al. (1998, except  $T_p$  where we used our median time value). The pulsation and orbital velocity curves are displayed in Fig. 11, and our fitted parameters in Table 11. We used the same fitting formalism as for FF Aql. Our revised orbit is in good agreement with previous works (Böhm-Vitense et al. 1998; Lloyd Evans 1982), with a final r.m.s. of the residual of  $230 \text{ m s}^{-1}$ . However, the orbital period of 1362 days given by Petterson et al. (2004) is not in agreement, and the fit does not converge if we use this value as first guess. As a first test, we re-derived the pulsation and orbital parameters using only the RVs from Petterson et al. (2004, post-1997 data only). We found a period of 1323.4 days, more consistent with our previous estimate, as for the other parameters, except the systemic velocity which is positively shifted by  $1 \text{ km s}^{-1}$ . A possible explanation for the orbital period mismatch

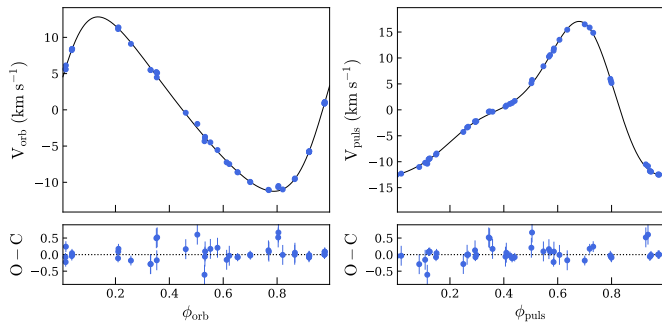


**Fig. 11.** Same as Fig. 5 but for V636 Sco.

**Table 11.** Final estimated parameters of the V636 Sco system.

Pulsation		
$P_{\text{puls}}$ (days)	$6.79703 \pm 0.00002$	
$T_0$ (JD) <sup>a</sup>	2 434 906.47	
$A_1$ (km s <sup>-1</sup> )	$-9.44 \pm 0.45$	
$B_1$ (km s <sup>-1</sup> )	$-7.77 \pm 0.57$	
$A_2$ (km s <sup>-1</sup> )	$-4.36 \pm 0.35$	
$B_2$ (km s <sup>-1</sup> )	$2.69 \pm 0.50$	
$A_3$ (km s <sup>-1</sup> )	$0.99 \pm 0.21$	
$B_3$ (km s <sup>-1</sup> )	$1.11 \pm 0.21$	
$A_4$ (km s <sup>-1</sup> )	$0.30 \pm 0.06$	
$B_4$ (km s <sup>-1</sup> )	$-0.04 \pm 0.09$	
Orbit		
	Bo98 <sup>b</sup>	This work
$P_{\text{orb}}$ (days)	$1323.6 \pm 1.2$	$1320.6 \pm 1.3$
$T_p$ (JD)	$2\,430\,411.4 \pm 20.9$	$2\,456\,865.5 \pm 5.7$
$e$	$0.213 \pm 0.020$	$0.250 \pm 0.004$
$\omega$ (°)	$294 \pm 52$	$288.0 \pm 2.5$
$K_1$ (km s <sup>-1</sup> )	$12.19 \pm 0.22$	$11.98 \pm 0.06$
$v_\gamma$ (km s <sup>-1</sup> )	$9.09 \pm 0.17$	$9.0 \pm 0.06$
$a_1 \sin i$ (au)	$1.451 \pm 0.027$	$1.409 \pm 0.007$
$f(M)$ ( $M_\odot$ )	$0.230 \pm 0.013$	$0.214 \pm 0.003$

**Notes.** <sup>(a)</sup> Not fitted. <sup>(b)</sup> Böhm-Vitense et al. (1998).

is the pulsation period change which was not taken into account in Peterson et al. (2004) as they combined their data with imprecise old measurements (Stibbs 1955; Lloyd Evans 1968).

**AH Vel:** We did not detect any companion from our interferometric observations. However, our derived detection limits allow us to set an upper limit on the spectral type. According to our estimate of  $\Delta H_{3\sigma} = 5.3$  mag, we can rule out any component earlier than an A0V star within 50 mas.

New spectroscopic observations were also collected from 2012 to 2015 with the spectrograph HARPS and CORALIE (see Appendix B and Tables B.1-B.11). As for BP Cir, we first analysed our RVs by fitting only the pulsation of the Cepheid with Fourier series. The curve is displayed in Fig. 7, and the fitted parameters are listed in Table 7. Although we see no trend in the residual (r.m.s of  $0.28$  km s<sup>-1</sup>), we calculated the periodogram. We did not find any significant periodic signal in the power spectrum, the highest peak having a FAP of  $\sim 8\%$ . Ignoring possible period change, we performed the same analysis by including old RV measurements (Lloyd Evans 1968; Gieren 1977; Lloyd Evans 1980; Bersier 2002) to have a longer time span. We iden-

tified a significant peak (with a FAP  $< 0.1\%$ ) at a period of  $\sim 7060$  days. We also noticed two other peaks with significant levels at periods  $\sim 3100$  and  $\sim 14000$  days (with FAP  $< 1\%$ ). We stress that such analysis assume a zero eccentricity and ignore pulsation period change. This preliminary  $\sim 7060$  days orbital period needs confirmation with additional high-precision contemporaneous RV measurements.

## 5. Conclusion

We reported new multi-telescope interferometric observations for 16 Galactic classical Cepheids. We used the CANDID algorithm (Gallenne et al. 2015) to search for high-contrast companions within a relative distance to the Cepheid of 50 mas. We also report detection limit for undetected components (secondary or tertiary).

The components orbiting U Aql, BP Cir and S Mus are clearly detected. They are located at projected separations of 2-40 mas, and with flux ratios in the range 0.4-3.5%. We have preliminary detections for FF Aql, Y Car, BG Cru, X Sgr, V350 Sgr and V636 Sco, but a confirmation is needed due to our low detections levels or several possible locations. For U Car, YZ Car, T Mon, R Mus, S Nor, W Sgr and AH Vel we have no detection, however we set upper limits on the companion' spectral types. Upper limits on the spectral type of possible tertiary component were also estimated for the other targets.

We present preliminary complete astrometric and spectroscopic orbits for the Cepheids U Aql and S Mus, combining astrometric and single-line velocity measurements. We derived preliminary dynamical masses for these Cepheids assuming a distance from a P-L relation (Storm et al. 2011). We found  $M = 4.97 \pm 0.62 M_\odot$  and  $M = 4.63 \pm 0.99 M_\odot$ , respectively for U Aql and S Mus.

Based on new high-precision spectroscopic observations with the SOPHIE, CORALIE and HARPS spectrographs, we revised the pulsation and spectroscopic orbital parameters for FF Aql, YZ Car, W Sgr, V350 Sgr, and V636 Sco, while only the pulsation parameters of BP Cir, BG Cru, S Nor and AH Vel were updated.

Our interferometric observations also provided angular diameter measurements for all targets, and can be used for instance in a Baade-Wesselink method analysis (see e.g. Kervella et al. 2004; Gallenne et al. 2012; Breifelder et al. 2016).

Our interferometric program is promising to independently and accurately determine the mass and distance of Cepheids, as demonstrated by Gallenne et al. (2018a) who determined the distance of the Cepheid V1334 Cyg at a 1% accuracy level, providing the most accurate independent distance for a Cepheid. They also derived the mass of both components at  $< 3\%$  precision, which is also unique for a Galactic Cepheid. We now have additional Cepheids for which we detected the companion and measured their astrometric position (U Aql, RT Aur, AX Cir, BP Cir, S Mus, and AW Per, Gallenne et al. 2015, 2014b, 2013). The same analysis as that of V1334 Cyg can be applied if we have RVs for the companions. An astrometric follow-up is on-going to secure a better orbital coverage of these systems, and perform a combined fit with RV measurements.

**Acknowledgements.** The authors would like to thank the CHARA Array and Mount Wilson Observatory staff for their support. The CHARA Array is supported by the National Science Foundation under Grant No. AST-1211929, AST-1411654, AST-1636624, and AST-1715788. Institutional support has been provided from the GSU College of Arts and Sciences and the GSU Office of the Vice President for Research and Economic Development. The authors also thank all the people involved in the VLTI project. We acknowledge the support of the French Agence Nationale de la Recherche (ANR-15-CE31-0012-

01, project Unlock-Cepheids). WG and GP gratefully acknowledge financial support from the BASAL Centro de Astrofísica y Tecnologías Afines (CATA, AFB-170002). WG also acknowledges financial support from the Millennium Institute of Astrophysics (MAS) of the Iniciativa Científica Milenio del Ministerio de Economía, Fomento y Turismo de Chile (project IC120009). We acknowledge financial support from the Programme National de Physique Stellaire (PNPS) of CNRS/INSU, France. Support from the Polish National Science Centre grants MAESTRO UMO-2017/26/A/ST9/00446 and from the IdP II 2015 0002 64 grant of the Polish Ministry of Science and Higher Education is also acknowledged. The research leading to these results has received funding from the European Research Council (ERC) under the European Union's Horizon 2020 research and innovation programme (grant agreement No. 695099 and 639889). NRE acknowledges support from the Chandra X-ray Center NASA (contract NAS8-03060) and the HST grants GO-13454.001-A and GO-14194.002. JDM acknowledges HST/STScI grant support: HST-GO-13454.07-A, HST -GO-13841.006-A, HST-GO-14194.008-A. This work is based upon observations obtained with the Georgia State University Center for High Angular Resolution Astronomy Array at Mount Wilson Observatory. BP acknowledges financial support from the Polish National Science Center grant SONATA 2014/15/D/ST9/02248. This research is based on observations made with the SOPHIE spectrograph on the 1.93-m telescope at Observatoire de Haute-Provence (program IDs 13A.PNPS.GALL, 14A.PNPS.GALL, 15A.PNPS.GALL, 13B.PNPS.KER, 16B.PNPS.KER) and the CORALIE spectrograph on the Euler telescope at La Silla Observatory (program IDs CNTAC CN2013A, CN2014A and CN2015A). The Swiss 1.2 m Euler telescope is supported by the Swiss National Science Foundation. This research is based on observations made with the Mercator Telescope, operated on the island of La Palma by the Flemish Community, at the Spanish Observatorio del Roque de los Muchachos of the Instituto de Astrofísica de Canarias. HERMES is supported by the Fund for Scientific Research of Flanders (FWO), Belgium; the Research Council of K.U.Leuven, Belgium; the Fonds National de la Recherche Scientifique (F.R.S.-FNRS), Belgium; the Royal Observatory of Belgium; the Observatoire de Genève, Switzerland, and the Thüringer Landessternwarte, Tautenburg, Germany.

## References

- Abt, H. A. 1959, *ApJ*, 130, 769
- Albrow, M. D. & Cottrell, P. L. 1996, *MNRAS*, 280, 917
- Anderson, R. I. 2014, *A&A*, 566, L10
- Anderson, R. I., Casertano, S., Riess, A. G., et al. 2016a, *ApJS*, 226, 18
- Anderson, R. I., Ekström, S., Georgy, C., et al. 2014, *A&A*, 564, A100
- Anderson, R. I., Saio, H., Ekström, S., Georgy, C., & Meynet, G. 2016b, *A&A*, 591, A8
- Arellano-Ferro, A. & Madore, B. F. 1985, *The Observatory*, 105, 207
- Babel, J., Burki, G., Mayor, M., Chmielewski, Y., & Waelkens, C. 1989, *A&A*, 216, 125
- Balona, L. A. 1981, *The Observatory*, 101, 205
- Balona, L. A. 1983, *The Observatory*, 103, 163
- Benedict, G. F., McArthur, B. E., Feast, M. W., et al. 2007, *AJ*, 133, 1810
- Berdnikov, L. N. 2008, *VizieR Online Data Catalog: II/285*, originally published in: *Sternberg Astronomical Institute, Moscow*, 2285
- Bersier, D. 2002, *ApJS*, 140, 465
- Bersier, D., Burki, G., Mayor, M., & Duquennoy, A. 1994, *A&AS*, 108, 25
- Boffin, H. M. J., Hillen, M., Berger, J. P., et al. 2014, *A&A*, 564, A1
- Bohm-Vitense, E. 1986, *ApJ*, 303, 262
- Bohm-Vitense, E., Clark, M., Cottrell, P. L., & Wallerstein, G. 1990, *AJ*, 99, 353
- Bohm-Vitense, E., Evans, N. R., Carpenter, K., et al. 1998, *ApJ*, 505, 903
- Bohm-Vitense, E., Evans, N. R., Carpenter, K., et al. 1997, *AJ*, 114, 1176
- Böhm-Vitense, E. & Proffitt, C. 1985, *ApJ*, 296, 175
- Böhm-Vitense, E., Remage Evans, N., Carpenter, K., Beck-Winchatz, B., & Robinson, R. 1997, *ApJ*, 477, 916
- Bonneau, D., Clausse, J.-M., Delfosse, X., et al. 2006, *A&A*, 456, 789
- Bonneau, D., Delfosse, X., Mourard, D., et al. 2011, *A&A*, 535, A53
- Bono, G., Caputo, F., & Castellani, V. 2006, *Mem. Soc. Astron. Italiana*, 77, 207
- Bono, G., Groenewegen, M. A. T., Marconi, M., & Caputo, F. 2002, *ApJ*, 574, L33
- Bouchy, F. & Sophie Team. 2006, in *Tenth Anniversary of 51 Peg-b: Status of and prospects for hot Jupiter studies*, ed. L. Arnold, F. Bouchy, & C. Moutou, 319–325
- Breitfelder, J., Mérand, A., Kervella, P., et al. 2016, *A&A*, 587, A117
- Coulson, I. M. 1983a, *MNRAS*, 203, 925
- Coulson, I. M. 1983b, *MNRAS*, 205, 1135
- Coulson, I. M. & Caldwell, J. A. R. 1985, *South African Astron. Observ. Circ.*, 9, 5
- Cutri, R. M., Skrutskie, M. F., van Dyk, S., et al. 2003, *VizieR Online Data Catalog*, 2246, 0
- Derekas, A., Plachy, E., Molnár, L., et al. 2017, *MNRAS*, 464, 1553
- Evans, N. R. 1990, *PASP*, 102, 551
- Evans, N. R. 1991, *ApJ*, 372, 597
- Evans, N. R. 1992a, *ApJ*, 384, 220
- Evans, N. R. 1992b, *ApJ*, 389, 657
- Evans, N. R. 1992c, *ApJ*, 385, 680
- Evans, N. R. 1994, *ApJ*, 436, 273
- Evans, N. R. 2011, in *IAU Symposium, Vol. 272*, IAU Symposium, ed. C. Neiner, G. Wade, G. Meynet, & G. Peters, 537–538
- Evans, N. R. 2013, in *Astrophysics and Space Science Proceedings, Vol. 31, Stellar Pulsations: Impact of New Instrumentation and New Insights*, ed. J. C. Suárez, R. Garrido, L. A. Balona, & J. Christensen-Dalsgaard, 95
- Evans, N. R., Berdnikov, L., Gorynya, N., Rastorguev, A., & Eaton, J. 2011, *AJ*, 142, 87
- Evans, N. R., Boehm-Vitense, E., Carpenter, K., Beck-Winchatz, B., & Robinson, R. 1998, *ApJ*, 494, 768
- Evans, N. R., Bond, H. E., Schaefer, G. H., et al. 2013, *AJ*, 146, 93
- Evans, N. R. & Butler, J. 1993, *PASP*, 105, 915
- Evans, N. R., Carpenter, K., Robinson, R., et al. 1999, *ApJ*, 524, 379
- Evans, N. R., Carpenter, K. G., Robinson, R., Kienzie, F., & Dekas, A. E. 2005, *AJ*, 130, 789
- Evans, N. R., Karovska, M., Bond, H. E., et al. 2018a, *ApJ*, 863, 187
- Evans, N. R. & Lyons, R. W. 1994, *AJ*, 107, 2164
- Evans, N. R., Massa, D., Fullerton, A., Sonneborn, G., & Iping, R. 2004, in *Astronomical Society of the Pacific Conference Series, Vol. 310, IAU Colloq. 193: Variable Stars in the Local Group*, ed. D. W. Kurtz & K. R. Pollard, 377
- Evans, N. R., Massa, D., & Proffitt, C. 2009, *AJ*, 137, 3700
- Evans, N. R., Massa, D., & Teays, T. J. 1994, *AJ*, 108, 2251
- Evans, N. R., Proffitt, C., Carpenter, K. G., et al. 2018b, *ApJ*, 866, 30
- Evans, N. R., Schaefer, G. H., Bond, H. E., et al. 2008, *AJ*, 136, 1137
- Evans, N. R., Szabó, R., Derekas, A., et al. 2015, *MNRAS*, 446, 4008
- Evans, N. R., Welch, D. L., Scarfe, C. D., & Teays, T. J. 1990, *AJ*, 99, 1598
- Feast, M. W. 1967, *MNRAS*, 136, 141
- Foreman-Mackey, D., Hogg, D. W., Lang, D., & Goodman, J. 2013, *PASP*, 125, 306
- Gaia Collaboration, Brown, A. G. A., Vallenari, A., et al. 2018, *A&A*, 616, A1
- Gallenne, A., Kervella, P., Evans, N. R., et al. 2018a, *ApJ*, 867, 121
- Gallenne, A., Kervella, P., Mérand, A., et al. 2014a, *A&A*, 567, A60
- Gallenne, A., Kervella, P., Mérand, A., et al. 2012, *A&A*, 541, A87
- Gallenne, A., Mérand, A., Kervella, P., et al. 2014b, *A&A*, 561, L3
- Gallenne, A., Mérand, A., Kervella, P., et al. 2015, *A&A*, 579, A68
- Gallenne, A., Monnier, J. D., Mérand, A., et al. 2013, *A&A*, 552, A21
- Gallenne, A., Pietrzyński, G., Graczyk, D., et al. 2018b, *A&A*, 616, A68
- Gieren, W. 1977, *A&AS*, 28, 193
- Gieren, W. 1982, *ApJS*, 49, 1
- Gieren, W., Pilecki, B., Pietrzyński, G., et al. 2014, *ApJ*, 786, 80
- Gieren, W. P. 1989, *A&A*, 216, 135
- Gillet, D. 2014, *A&A*, 568, A72
- Gorynya, N. A., Samus, N. N., Berdnikov, L. N., Rastorguev, A. S., & Sachkov, M. E. 1995, *IBVS*, 4199
- Gorynya, N. A., Samus, N. N., Sachkov, M. E., et al. 1998, *Astronomy Letters*, 24, 815
- Groenewegen, M. A. T. 2008, *A&A*, 488, 25
- Haguenauer, P., Alonso, J., Bourget, P., et al. 2010, in *SPIE Conference Series, Vol. 7734*
- Keller, S. C. 2008, *ApJ*, 677, 483
- Kervella, P., Bigot, L., Gallenne, A., & Thévenin, F. 2017, *A&A*, 597, A137
- Kervella, P., Gallenne, A., Evans, N. R., et al. 2018, *A&A*, in press [e-print:]
- Kervella, P., Nardetto, N., Bersier, D., Mourard, D., & Coudé du Foresto, V. 2004, *A&A*, 416, 941
- Kraus, A. L. & Ireland, M. J. 2012, *ApJ*, 745, 5
- Le Bouquin, J.-B., Berger, J.-P., Lazareff, B., et al. 2011, *A&A*, 535, A67
- Leavitt, H. S. 1908, *Annals of Harvard College Observatory*, 60, 87
- Leavitt, H. S. & Pickering, E. C. 1912, *Harvard College Observatory Circular*, 173, 1
- Li Causi, G., Antonucci, S., Bono, G., et al. 2013, *A&A*, 549, A64
- Lloyd Evans, T. 1968, *MNRAS*, 141, 109
- Lloyd Evans, T. 1980, *SAAO Circ.*, 1, 257
- Lloyd Evans, T. 1982, *MNRAS*, 199, 925
- Mariska, J. T., Doschek, G. A., & Feldman, U. 1980, *ApJ*, 242, 1083
- Mermilliod, J. C., Mayor, M., & Burki, G. 1987, *A&AS*, 70, 389
- Monnier, J. D., Anderson, M., Baron, F., et al. 2010, in *SPIE Conference Series, ed. W. C. Danchi, F. Delplanck, & J. K. Rajagopal, Vol. 7734, 77340G–77340G–12*
- Monnier, J. D., Berger, J.-P., Millan-Gabet, R., & ten Brummelaar, T. A. 2004, in *SPIE Conference Series, ed. W. A. Traub, Vol. 5491, 1370*
- Monnier, J. D., Che, X., Zhao, M., et al. 2012, *ApJ*, 761, L3
- Monnier, J. D., Zhao, M., Pedretti, E., et al. 2007, *Science*, 317, 342
- Moore, J. H. 1929, *PASP*, 41, 56

- Morgan, B. L., Beddoes, D. R., Scaddan, R. J., & Dainty, J. C. 1978, *MNRAS*, 183, 701
- Neilson, H. R., Cantiello, M., & Langer, N. 2011, *A&A*, 529, L9
- Neilson, H. R. & Ignace, R. 2014, *A&A*, 563, L4
- Neilson, H. R., Schneider, F. R. N., Izzard, R. G., Evans, N. R., & Langer, N. 2015, *A&A*, 574, A2
- Pecaut, M. J. & Mamajek, E. E. 2013, *ApJS*, 208, 9
- Pecaut, M. J., Mamajek, E. E., & Bubar, E. J. 2012, *ApJ*, 746, 154
- Pepe, F., Mayor, M., Rupprecht, G., et al. 2002, *The Messenger*, 110, 9
- Petterson, O. K. L., Cottrell, P. L., & Albrow, M. D. 2004, *MNRAS*, 350, 95
- Petterson, O. K. L., Cottrell, P. L., Albrow, M. D., & Fokin, A. 2005, *MNRAS*, 362, 1167
- Pietrzyński, G., Thompson, I. B., Gieren, W., et al. 2010, *Nature*, 468, 542
- Pilecki, B., Gieren, W., Pietrzyński, G., et al. 2018, *ApJ*, 862, 43
- Pilecki, B., Graczyk, D., Pietrzyński, G., et al. 2013, *MNRAS*, 436, 953
- Prada Moroni, P. G., Gennaro, M., Bono, G., et al. 2012, *ApJ*, 749, 108
- Queloz, D., Mayor, M., Udry, S., et al. 2001, *The Messenger*, 105, 1
- Raskin, G., van Winckel, H., Hensberge, H., et al. 2011, *A&A*, 526, A69
- Samus, N. N., Kazarovets, E. V., Durlevich, O. V., Kireeva, N. N., & Pastukhova, E. N. 2017, *Astronomy Reports*, 61, 80
- Sanford, R. F. 1930, *Contributions from the Mount Wilson Observatory / Carnegie Institution of Washington*, 404, 1
- Slovak, M. H., van Citters, G. W., & Barnes, III, T. G. 1979, *PASP*, 91, 840
- Soubiran, C., Jasniewicz, G., Chemin, L., et al. 2013, *A&A*, 552, A64
- Stibbs, D. W. N. 1955, *MNRAS*, 115, 363
- Stobie, R. S. 1970, *MNRAS*, 148, 1
- Stobie, R. S. & Balona, L. A. 1979a, *MNRAS*, 189, 627
- Stobie, R. S. & Balona, L. A. 1979b, *MNRAS*, 189, 641
- Storm, J., Gieren, W., Fouqué, P., et al. 2011, *A&A*, 534, A94
- Szabados, L. 1977, *Commun. of the Konkoly Observatory Hungary*, 70, 1
- Szabados, L. 1989, *Commun. of the Konkoly Observatory Hungary*, 94, 1
- Szabados, L. 1990, *MNRAS*, 242, 285
- Szabados, L. 1991, *Commun. of the Konkoly Observatory Hungary*, 96, 123
- ten Brummelaar, T. A., McAlister, H. A., Ridgway, S. T., et al. 2005, *ApJ*, 628, 453
- Udry, S., Mayor, M., & Queloz, D. 1999, in *ASPCS, Vol. 185, IAU Colloq. 170: Precise Stellar Radial Velocities*, ed. J. B. Hearnshaw & C. D. Scarfe, 367
- Usenko, I. A., Kniazev, A. Y., Berdnikov, L. N., Fokin, A. B., & Kravtsov, V. V. 2014, *Astronomy Letters*, 40, 435
- van Leeuwen, F., Feast, M. W., Whitelock, P. A., & Laney, C. D. 2007, *MNRAS*, 379, 723
- VanderPlas, J., Connolly, A. J., Ivezić, Z., & Gray, A. 2012, in *Proceedings of Conference on Intelligent Data Understanding (CIDU)*, pp. 47–54
- Walraven, J. H., Tinbergen, J., & Walraven, T. 1964, *Bull. Astron. Inst. Netherlands*, 17, 520
- Welch, D. L., Evans, N. R., Lyons, R. W., et al. 1987, *PASP*, 99, 610
- Wilson, T. D., Carter, M. W., Barnes, III, T. G., van Citters, Jr., G. W., & Moffett, T. J. 1989, *ApJS*, 69, 951

## Appendix A: Parameters of the calibrators used for MIRC and PIONIER interferometric observations

The parameters of the calibrators we used are listed in Table A.1. They were collected with the SearchCal software.

## Appendix B: New radial velocities from the CORALIE, SOPHIE, HARPS and HERMES spectrographs

We collected several spectra from 2012 to 2017 with the fibered SOPHIE spectrograph ( $R \sim 75\,000$  [Bouchy & Sophie Team 2006](#)), mounted on the 1.93 m telescope of the Observatoire de Haute Provence (France), the CORALIE spectrograph ( $R \sim 60\,000$  [Queloz et al. 2001](#)) at the Swiss 1.2 m Euler telescope located at La Silla Observatory, the HARPS spectrograph ( $R \sim 115\,000$  [Pepe et al. 2002](#)) mounted on the 3.6 m ESO telescope at La Silla Observatory, and the HERMES spectrograph ( $R \sim 85\,000$  [Raskin et al. 2011](#)) mounted on the Flemish 1.2 m telescope of the Roque de los Muchachos Observatory. These four instruments cover the visible wavelength. Exposure times of a few minutes allowed a signal-to-noise ratio  $> 10$  per pixel at 550nm. All data were reduced using the dedicated instrument pipeline.

Radial velocities were estimated using the cross-correlation method. We created our own weighted binary mask by selecting unblended lines from high-resolution synthetic spectra ( $R \sim 120\,000$ ) covering the wavelength range 4500-6800 Å. The cross-correlation function is then fitted by a Gaussian whose minimum value gives an estimate of the RV. Uncertainties include photon noise and internal drift. Zero point difference was set to the HARPS or CORALIE system (when there are no HARPS data) following the table of [Soubiran et al. \(2013\)](#) for CORALIE, HARPS and SOPHIE, and [Gallenne et al. \(2018a\)](#) for HERMES. RV measurements are listed from Table B.2 to B.3 (without correction for the zero point).

**Table A.1.** Calibrators used for our observations.

HD	Sp. type	$V$ (mag)	$H$ (mag)	$\theta_{UD}$ (mas)	HD	Sp. type	$V$ (mag)	$H$ (mag)	$\theta_{UD}$ (mas)
43299	K3III-IV	6.84	4.44	$0.720 \pm 0.051$	132209	A9/F0IV/V	6.56	5.83	$0.248 \pm 0.017$
45317	K0III	6.87	4.60	$0.628 \pm 0.045$	144230	K2III	8.67	5.41	$0.465 \pm 0.011$
66080	G6III	7.44	5.48	$0.398 \pm 0.028$	145361	F2IV/V	5.77	4.89	$0.449 \pm 0.032$
70195	G8/K0III	7.08	5.08	$0.492 \pm 0.035$	145883	K2III	8.45	5.39	$0.457 \pm 0.010$
73075	K1III	7.34	5.16	$0.467 \pm 0.033$	146247	K2III	7.21	4.61	$0.653 \pm 0.046$
85253	K1(III)	8.69	–	$0.320 \pm 0.023$	147075	K1III	7.90	5.27	$0.465 \pm 0.033$
89517	K1/2III	8.59	5.87	$0.366 \pm 0.026$	147422	K0III	8.04	5.34	$0.445 \pm 0.011$
89839	F7V	7.64	6.47	$0.225 \pm 0.016$	148679	K0III	6.94	4.69	$0.609 \pm 0.043$
90074	G6III	6.35	4.52	$0.652 \pm 0.046$	149835	K0III	7.30	5.07	$0.499 \pm 0.035$
90246	K0III	8.25	5.82	$0.349 \pm 0.025$	151005	K0III	7.21	4.69	$0.595 \pm 0.042$
90980	K0III	6.74	4.42	$0.657 \pm 0.047$	151337	K0IV/V	7.38	5.39	$0.425 \pm 0.030$
92156	G0IV/V	8.03	6.73	$0.197 \pm 0.014$	152272	K1III	7.35	4.91	$0.555 \pm 0.039$
93307	G0V	7.78	6.45	$0.229 \pm 0.016$	154250	K0III	8.00	5.72	$0.365 \pm 0.026$
94256	K0III	7.95	5.73	$0.357 \pm 0.025$	154486	K2/3III	6.94	3.50	$1.056 \pm 0.015$
96068	G8III	6.52	4.37	$0.709 \pm 0.090$	155019	K1III	8.99	5.24	$0.475 \pm 0.034$
97744	K0/1III	8.30	5.93	$0.336 \pm 0.024$	156992	K3III	6.36	3.12	$1.240 \pm 0.017$
98692	K2III	7.45	4.99	$0.568 \pm 0.040$	159217	A0V	4.59	4.66	$0.373 \pm 0.026$
98732	K0III	7.02	4.95	$0.580 \pm 0.041$	159285	K1III	7.97	5.44	$0.416 \pm 0.030$
98897	G8III	6.63	4.31	$0.603 \pm 0.045$	159941	M0III	7.82	3.73	$1.081 \pm 0.015$
99048	K2III	7.13	4.28	$0.673 \pm 0.048$	160113	G5V	7.28	5.69	$0.333 \pm 0.024$
100078	K2III	7.33	4.19	$0.836 \pm 0.011$	162415	K5III	6.94	3.66	$1.003 \pm 0.072$
101805	F8V	6.47	5.30	$0.375 \pm 0.026$	163652	G8III	5.74	3.64	$0.900 \pm 0.064$
102534	K1III	6.76	4.66	$0.643 \pm 0.046$	166230	A8III	5.10	4.66	$0.409 \pm 0.029$
102969	G8III	7.66	5.28	$0.460 \pm 0.033$	166295	K2III/IV	6.68	2.94	$1.266 \pm 0.017$
105939	K0III	7.05	4.70	$0.601 \pm 0.043$	169236	K0III	6.14	3.69	$0.890 \pm 0.063$
107013	K1III	7.97	5.77	$0.343 \pm 0.024$	171960	K3III	7.29	3.50	$1.121 \pm 0.016$
107720	K1III	7.12	4.78	$0.586 \pm 0.042$	174774	K4III	7.56	3.83	$1.103 \pm 0.015$
109761	G6III	7.41	5.26	$0.442 \pm 0.031$	177067	K0III	6.91	4.64	$0.634 \pm 0.045$
110532	K0/1III	6.42	4.16	$0.783 \pm 0.011$	178218	K0III	6.88	4.55	$0.658 \pm 0.047$
110924	K0II/III	6.64	4.15	$0.745 \pm 0.053$	182807	F7V	6.20	4.93	$0.457 \pm 0.032$
112124	G8III	7.21	4.87	$0.536 \pm 0.038$	184985	F7V	5.45	4.42	$0.589 \pm 0.041$
115669	K2/3III	6.91	4.13	$0.766 \pm 0.055$	185124	F3IV/V	5.68	4.58	$0.515 \pm 0.036$
121901	F0/2III/IV	6.47	5.72	$0.284 \pm 0.020$	188844	K0III/IV	6.57	4.50	$0.660 \pm 0.047$
125136	K0III	7.44	5.27	$0.440 \pm 0.031$	196870	K0III	6.61	4.32	$0.685 \pm 0.049$
130551	F5V	8.75	5.96	$0.276 \pm 0.019$	198001	B9.5V	3.77	3.71	$0.510 \pm 0.036$

**Table B.1.** Radial velocity measurements of U Aql.

MJD (days)	RV (km s <sup>-1</sup> )	$\sigma_{RV}$ (km s <sup>-1</sup> )	Inst.
56213.985087	-3.15	0.11	HARPS
56239.989431	-14.08	0.13	HARPS
56241.017804	-9.62	0.12	HARPS
56448.452412	23.07	0.12	HARPS
56553.149712	15.01	0.11	HARPS
56908.128645	-5.14	0.12	HARPS
57635.059769	2.57	0.12	HARPS
57636.026251	13.93	0.15	HARPS
57901.307348	-0.37	0.11	HARPS
57902.184474	11.02	0.12	HARPS
57903.270561	18.38	0.16	HARPS
57916.219488	11.24	0.12	HARPS
56471.085989	0.01	0.12	SOPHIE
56472.078955	-9.35	0.11	SOPHIE
56473.031282	-4.13	0.11	SOPHIE
56474.075913	2.86	0.10	SOPHIE
56475.073713	6.28	0.10	SOPHIE
56476.039045	16.31	0.11	SOPHIE
56477.057247	28.52	0.14	SOPHIE
56557.801666	-0.03	0.10	SOPHIE
56558.863991	6.84	0.10	SOPHIE
56559.878414	11.18	0.11	SOPHIE
56560.831546	24.27	0.12	SOPHIE
56561.821282	25.15	0.14	SOPHIE
56562.862657	-8.40	0.12	SOPHIE
56814.104828	29.67	0.14	SOPHIE
56816.084294	-7.90	0.12	SOPHIE
56818.036831	3.23	0.10	SOPHIE
57179.053565	21.38	0.13	SOPHIE
57180.059515	17.09	0.14	SOPHIE
57181.057767	-12.90	0.12	SOPHIE
56399.324683	22.89	0.12	CORALIE
56400.321920	20.68	0.13	CORALIE
56461.289864	7.59	0.10	CORALIE
56461.417069	8.81	0.10	CORALIE
56462.285588	20.36	0.12	CORALIE
56462.411588	22.04	0.12	CORALIE
56462.424401	22.25	0.12	CORALIE
56750.368062	23.61	0.12	CORALIE
56750.379174	23.73	0.12	CORALIE
56750.390205	23.89	0.12	CORALIE
56751.364938	28.62	0.14	CORALIE
56751.376051	28.39	0.14	CORALIE
56751.387024	28.17	0.14	CORALIE
56826.390217	8.62	0.10	CORALIE
56826.401190	8.68	0.10	CORALIE
56826.412220	8.73	0.10	CORALIE
56826.423204	8.80	0.10	CORALIE
56827.397793	20.23	0.11	CORALIE
56827.408801	20.40	0.11	CORALIE
56827.419785	20.54	0.11	CORALIE
57135.350389	4.33	0.10	CORALIE
57135.363875	4.35	0.10	CORALIE
57136.347787	14.64	0.11	CORALIE
57137.372212	26.42	0.14	CORALIE
57473.393066	2.32	0.11	CORALIE
57476.419085	-22.77	0.11	CORALIE
57477.398320	-17.75	0.10	CORALIE

**Table B.2.** Radial velocity measurements of FF Aql.

MJD (days)	RV (km s <sup>-1</sup> )	$\sigma_{RV}$ (km s <sup>-1</sup> )	Inst.	MJD (days)	RV (km s <sup>-1</sup> )	$\sigma_{RV}$ (km s <sup>-1</sup> )	Inst.
56399.372658	-15.05	0.11	CORALIE	56446.118545	-27.33	0.11	SOPHIE
56400.369897	-15.04	0.11	CORALIE	56447.036907	-26.93	0.11	SOPHIE
56461.266962	-20.53	0.11	CORALIE	56447.041583	-26.90	0.11	SOPHIE
56462.238574	-12.98	0.11	CORALIE	56448.104962	-18.19	0.11	SOPHIE
56462.306712	-12.71	0.11	CORALIE	56449.111335	-12.52	0.12	SOPHIE
56750.401128	-23.07	0.11	CORALIE	57644.844908	-28.18	0.11	SOPHIE
56751.397916	-19.50	0.11	CORALIE	57650.786739	-18.38	0.11	SOPHIE
56826.298032	-20.93	0.11	CORALIE	56855.100210	-9.29	0.11	HERMES
56827.307666	-18.49	0.11	CORALIE	56856.044422	-4.94	0.11	HERMES
57135.333071	-19.57	0.11	CORALIE	56857.030988	-15.49	0.11	HERMES
57136.368934	-12.44	0.11	CORALIE	56858.028974	-20.61	0.11	HERMES
57137.346922	-4.65	0.11	CORALIE	56859.028970	-14.50	0.11	HERMES
57470.401531	-25.73	0.11	CORALIE	56860.039263	-5.82	0.11	HERMES
57472.399768	-12.02	0.11	CORALIE	56861.040693	-8.50	0.11	HERMES
57473.403685	-11.72	0.11	CORALIE	56862.042044	-20.34	0.11	HERMES
57476.412521	-16.04	0.11	CORALIE	56864.028492	-9.42	0.11	HERMES
57477.405108	-9.90	0.11	CORALIE	56865.033989	-4.88	0.11	HERMES
57478.417082	-19.10	0.11	CORALIE	56866.028913	-16.11	0.11	HERMES
57498.390839	-19.93	0.10	CORALIE	57178.049664	-4.67	0.11	HERMES
57500.395837	-14.09	0.11	CORALIE	57180.029113	-20.13	0.11	HERMES
57504.428585	-10.85	0.11	CORALIE	57181.025161	-13.44	0.10	HERMES
57507.391957	-19.65	0.10	CORALIE	57182.016061	-5.44	0.11	HERMES
57508.324257	-11.52	0.11	CORALIE	57183.018201	-9.02	0.11	HERMES
57508.409506	-11.28	0.11	CORALIE	57184.015859	-20.38	0.11	HERMES
57526.363465	-11.24	0.11	CORALIE	57185.010898	-17.70	0.10	HERMES
57529.360015	-23.38	0.11	CORALIE	57186.000617	-8.77	0.10	HERMES
57534.333270	-18.96	0.11	CORALIE	57188.001022	-16.84	0.11	HERMES
57536.358535	-17.40	0.11	CORALIE	57567.050781	-11.82	0.11	HERMES
57835.363211	-13.43	0.11	CORALIE	57568.069138	-24.06	0.11	HERMES
57840.389289	-19.25	0.11	CORALIE	57569.055557	-27.04	0.11	HERMES
57845.398729	-26.57	0.11	CORALIE	57571.125510	-11.85	0.11	HERMES
57848.406122	-12.93	0.11	CORALIE	57572.090768	-17.34	0.11	HERMES
57869.420962	-22.77	0.10	CORALIE	57573.108456	-27.59	0.11	HERMES
57870.394944	-14.23	0.11	CORALIE	57574.147203	-23.42	0.10	HERMES
57871.412147	-15.38	0.11	CORALIE	57998.851481	-23.18	0.11	HERMES
57872.418526	-27.64	0.11	CORALIE	57999.886736	-13.93	0.11	HERMES
57876.376142	-22.32	0.11	CORALIE	58000.894608	-12.18	0.11	HERMES
58228.406034	-6.22	0.11	CORALIE	58001.886619	-24.89	0.11	HERMES
58229.415646	-13.14	0.11	CORALIE	58024.923068	-26.40	0.11	HERMES
58230.399781	-21.85	0.11	CORALIE	58025.896626	-20.77	0.10	HERMES
58231.340071	-18.04	0.11	CORALIE	58032.877642	-20.52	0.11	HERMES
58235.321229	-20.78	0.11	CORALIE	58069.831394	-24.86	0.11	HERMES
58237.392442	-5.85	0.11	CORALIE	58070.832411	-17.81	0.10	HERMES

**Table B.3.** Radial velocity measurements of YZ Car.

MJD (days)	RV (km s <sup>-1</sup> )	$\sigma_{RV}$ (km s <sup>-1</sup> )	Inst.
56240.378977	4.72	0.10	HARPS
56448.004155	16.36	0.15	HARPS
56448.999019	11.49	0.14	HARPS
56450.012629	6.42	0.13	HARPS
56605.365482	-5.81	0.10	HARPS
56398.983650	-5.06	0.12	CORALIE
56399.992636	-7.80	0.11	CORALIE
56461.042669	7.99	0.11	CORALIE
56461.979525	11.12	0.11	CORALIE
56750.001563	-11.08	0.11	CORALIE
56751.001637	-7.34	0.12	CORALIE
56825.971994	3.81	0.12	CORALIE
56826.967563	6.39	0.13	CORALIE
57134.983140	20.87	0.12	CORALIE
57135.985212	23.26	0.13	CORALIE
57136.984309	24.46	0.13	CORALIE
57198.012720	-2.02	0.12	CORALIE

**Table B.4.** Radial velocity measurements of BP Cir.

MJD (days)	RV (km s <sup>-1</sup> )	$\sigma_{RV}$ (km s <sup>-1</sup> )	Inst.
56399.093613	-10.40	0.11	CORALIE
56399.394898	-11.05	0.11	CORALIE
56400.102809	-26.39	0.11	CORALIE
56400.392092	-24.16	0.11	CORALIE
56461.097700	-13.81	0.10	CORALIE
56462.100168	-20.29	0.11	CORALIE
56750.129817	-26.03	0.12	CORALIE
56750.147064	-26.15	0.12	CORALIE
56750.164299	-26.27	0.12	CORALIE
56751.126307	-15.76	0.11	CORALIE
56751.143808	-15.53	0.11	CORALIE
56751.161170	-15.31	0.11	CORALIE
56826.104945	-10.25	0.11	CORALIE
56826.122179	-10.26	0.11	CORALIE
56826.139470	-10.33	0.11	CORALIE
56827.101280	-26.03	0.11	CORALIE
56827.118525	-25.85	0.11	CORALIE
56827.135781	-25.71	0.11	CORALIE
57135.152884	-12.08	0.11	CORALIE
57135.264080	-11.07	0.11	CORALIE
57136.110904	-24.27	0.12	CORALIE
57136.221556	-26.12	0.12	CORALIE
57137.109560	-17.65	0.11	CORALIE
57137.220223	-16.09	0.11	CORALIE
57198.154736	-15.10	0.11	CORALIE
57198.244362	-17.66	0.12	CORALIE
56876.984618	-20.48	0.12	HARPS
56877.988780	-19.19	0.11	HARPS
56878.988466	-11.02	0.12	HARPS
56907.987903	-14.79	0.12	HARPS
56908.985107	-21.95	0.11	HARPS
56909.996458	-10.07	0.11	HARPS

**Table B.5.** Radial velocity measurements of BG Cru.

MJD (days)	RV (km s <sup>-1</sup> )	$\sigma_{RV}$ (km s <sup>-1</sup> )	Inst.
56399.020058	-17.80	0.16	CORALIE
56399.158116	-16.77	0.16	CORALIE
56400.028892	-16.07	0.17	CORALIE
56461.085840	-24.84	0.17	CORALIE
56461.122691	-24.98	0.17	CORALIE
56462.089207	-21.26	0.17	CORALIE
56462.108743	-21.11	0.17	CORALIE
56750.178391	-16.45	0.17	CORALIE
56750.183935	-16.40	0.17	CORALIE
56751.175225	-17.91	0.17	CORALIE
56751.180850	-17.97	0.17	CORALIE
56826.151628	-23.16	0.17	CORALIE
56826.157172	-23.13	0.17	CORALIE
56827.147936	-15.89	0.17	CORALIE
56827.153491	-15.87	0.17	CORALIE
57135.109433	-14.78	0.17	CORALIE
57136.065043	-23.58	0.17	CORALIE
57137.063637	-22.70	0.17	CORALIE
57198.081791	-16.55	0.17	CORALIE
56242.383128	-14.95	0.18	HARPS
56448.022480	-24.95	0.18	HARPS
56449.009933	-18.75	0.18	HARPS
56450.003818	-14.98	0.18	HARPS

**Table B.6.** Radial velocity measurements of S Mus.

MJD (days)	RV (km s <sup>-1</sup> )	$\sigma_{RV}$ (km s <sup>-1</sup> )	Inst.
56399.031006	28.65	0.14	CORALIE
56400.040077	24.12	0.14	CORALIE
56460.979983	-1.28	0.11	CORALIE
56462.000067	1.23	0.11	CORALIE
56750.090093	-13.66	0.12	CORALIE
56750.108184	-13.59	0.12	CORALIE
56751.086165	-10.41	0.11	CORALIE
56751.104279	-10.34	0.11	CORALIE
56826.060596	2.91	0.12	CORALIE
56826.078744	2.66	0.12	CORALIE
56827.056896	-2.27	0.12	CORALIE
56827.075009	-2.24	0.12	CORALIE
57135.095919	-22.36	0.12	CORALIE
57136.051396	-29.08	0.12	CORALIE
57137.049998	-26.31	0.11	CORALIE
57198.069001	-18.45	0.11	CORALIE
57198.110956	-18.13	0.11	CORALIE
56241.387451	-10.05	0.11	HARPS
56242.380878	-2.81	0.11	HARPS
56448.015262	24.85	0.16	HARPS
56449.007513	7.67	0.14	HARPS
56450.007856	-2.92	0.13	HARPS
56876.979793	5.44	0.12	HARPS
56876.979793	5.44	0.12	HARPS
56877.984082	5.75	0.12	HARPS
56877.984082	5.75	0.12	HARPS
56878.984443	5.64	0.12	HARPS
56878.984443	5.64	0.12	HARPS
57902.192804	5.01	0.12	HARPS
57916.029102	29.48	0.16	HARPS
58098.313410	-0.92	0.12	HARPS
58139.324547	-13.92	0.14	HARPS
58140.194042	-26.83	0.13	HARPS
58141.169979	-27.44	0.12	HARPS

**Table B.7.** Radial velocity measurements of S Nor.

MJD (days)	RV (km s <sup>-1</sup> )	$\sigma_{RV}$ (km s <sup>-1</sup> )	Inst.
56399.195452	-1.50	0.10	CORALIE
56400.190823	8.14	0.10	CORALIE
56461.180856	24.03	0.15	CORALIE
56462.178882	8.36	0.13	CORALIE
56750.225028	-2.69	0.11	CORALIE
56750.237714	-2.58	0.11	CORALIE
56750.250377	-2.45	0.11	CORALIE
56751.221880	7.03	0.10	CORALIE
56751.234543	7.15	0.10	CORALIE
56751.247229	7.29	0.10	CORALIE
56826.200692	-2.44	0.11	CORALIE
56826.212405	-2.46	0.11	CORALIE
56826.224175	-2.47	0.11	CORALIE
56827.201646	-8.98	0.12	CORALIE
56827.214366	-8.99	0.12	CORALIE
56827.227028	-8.99	0.12	CORALIE
57135.196163	9.19	0.13	CORALIE
57136.152244	-2.20	0.12	CORALIE
57137.150896	-2.54	0.11	CORALIE
57198.201542	-8.07	0.11	CORALIE
56210.992794	-2.18	0.11	HARPS
56448.031120	-0.84	0.10	HARPS
56449.016947	8.78	0.10	HARPS
56449.996498	18.04	0.12	HARPS
57634.991198	-2.03	0.12	HARPS
57635.989614	-2.72	0.12	HARPS
57901.123581	-3.98	0.11	HARPS
57901.223692	-3.10	0.10	HARPS
57902.164485	5.89	0.10	HARPS
57902.202431	6.27	0.10	HARPS
57903.220158	16.09	0.11	HARPS
57916.106421	1.25	0.13	HARPS
58139.373600	20.48	0.15	HARPS
58140.366871	2.52	0.13	HARPS
58141.363640	-3.10	0.11	HARPS
58146.310875	8.74	0.10	HARPS
58148.394062	24.46	0.15	HARPS

**Table B.8.** Radial velocity measurements of W Sgr.

MJD (days)	RV (km s <sup>-1</sup> )	$\sigma_{RV}$ (km s <sup>-1</sup> )	Inst.
56877.006483	-19.53	0.14	HARPS
56878.004557	-42.93	0.12	HARPS
56879.003313	-38.79	0.11	HARPS
56908.139825	-41.83	0.12	HARPS
56399.247308	-41.59	0.12	CORALIE
56400.243681	-40.64	0.11	CORALIE
56461.166435	-39.31	0.11	CORALIE
56462.164196	-34.06	0.10	CORALIE
56750.314961	-36.06	0.11	CORALIE
56750.320587	-36.02	0.10	CORALIE
56751.312083	-30.64	0.10	CORALIE
56751.317686	-30.60	0.10	CORALIE
56826.284416	-36.11	0.10	CORALIE
56826.289832	-36.08	0.10	CORALIE
56827.293751	-30.59	0.10	CORALIE
56827.299353	-30.55	0.10	CORALIE
57135.248675	-20.91	0.13	CORALIE
57136.206267	-44.04	0.12	CORALIE
57137.204904	-40.25	0.11	CORALIE
57198.274594	-38.56	0.11	CORALIE
57568.076693	-18.37	0.12	HERMES
57569.063800	-45.39	0.11	HERMES
57572.099017	-31.47	0.10	HERMES
57573.116228	-28.28	0.10	HERMES
57574.084807	-15.81	0.11	HERMES
57627.855429	-8.93	0.12	HERMES
57628.863024	-19.42	0.12	HERMES
57629.850733	-45.49	0.11	HERMES
57630.860779	-41.76	0.11	HERMES
57635.845838	-7.05	0.13	HERMES
57999.854550	-8.23	0.12	HERMES
58001.862346	-42.47	0.11	HERMES
58002.855074	-40.57	0.11	HERMES
58026.818757	-34.08	0.10	HERMES
58239.173008	-34.66	0.10	HERMES
58246.104342	-38.20	0.11	HERMES
58247.170152	-32.77	0.10	HERMES
58248.155015	-28.62	0.10	HERMES

**Table B.9.** Radial velocity measurements of V350 Sgr.

MJD (days)	RV (km s <sup>-1</sup> )	$\sigma_{RV}$ (km s <sup>-1</sup> )	Inst.
56399.281661	10.44	0.11	CORALIE
56400.278886	20.66	0.12	CORALIE
56461.344731	18.44	0.11	CORALIE
56461.394616	18.99	0.11	CORALIE
56462.385830	28.46	0.12	CORALIE
56750.333340	23.09	0.11	CORALIE
56750.349846	23.26	0.11	CORALIE
56751.330291	32.30	0.13	CORALIE
56751.346797	32.48	0.13	CORALIE
56826.312569	6.92	0.11	CORALIE
56826.329097	7.07	0.11	CORALIE
56827.322199	17.69	0.11	CORALIE
56827.338704	17.86	0.11	CORALIE
57135.291045	-3.00	0.12	CORALIE
57136.258205	6.61	0.11	CORALIE
57136.279295	6.83	0.11	CORALIE
57137.256942	16.85	0.12	CORALIE
57137.278020	17.04	0.12	CORALIE
57198.290947	7.36	0.11	CORALIE
56877.010494	-0.99	0.13	HARPS
56878.009348	7.28	0.12	HARPS
56879.007162	17.93	0.12	HARPS
56908.010120	-1.39	0.13	HARPS
56909.004039	7.05	0.12	HARPS
56910.020588	18.00	0.12	HARPS

**Table B.10.** Radial velocity measurements of V636 Sco.

MJD (days)	RV (km s <sup>-1</sup> )	$\sigma_{RV}$ (km s <sup>-1</sup> )	Inst.
56876.996143	16.46	0.13	HARPS
56877.977498	26.24	0.14	HARPS
56878.977834	29.78	0.16	HARPS
56908.004614	4.81	0.14	HARPS
56909.009721	8.97	0.13	HARPS
56910.013893	15.28	0.13	HARPS
56399.218154	-8.14	0.12	CORALIE
56400.213531	-1.90	0.12	CORALIE
56461.202289	-4.18	0.12	CORALIE
56462.255361	0.20	0.12	CORALIE
56750.265874	9.22	0.14	CORALIE
56750.280933	8.82	0.14	CORALIE
56750.295981	8.43	0.14	CORALIE
56751.262801	-8.49	0.13	CORALIE
56751.277952	-8.55	0.13	CORALIE
56751.293081	-8.60	0.13	CORALIE
56826.239611	-2.58	0.13	CORALIE
56826.252690	-2.60	0.13	CORALIE
56826.265907	-2.61	0.13	CORALIE
56827.244015	0.45	0.12	CORALIE
56827.259130	0.54	0.12	CORALIE
56827.274188	0.62	0.12	CORALIE
57135.218268	21.59	0.12	CORALIE
57136.176623	30.80	0.13	CORALIE
57137.175246	36.07	0.15	CORALIE
57198.224645	34.78	0.15	CORALIE

**Table B.11.** Radial velocity measurements of AH Vel.

MJD (days)	RV (km s <sup>-1</sup> )	$\sigma_{RV}$ (km s <sup>-1</sup> )	Inst.
56398.967796	19.49	0.12	CORALIE
56399.103520	17.99	0.12	CORALIE
56399.976450	17.59	0.12	CORALIE
56460.953595	32.87	0.12	CORALIE
56460.963630	32.88	0.12	CORALIE
56461.958118	26.45	0.12	CORALIE
56461.963245	26.38	0.12	CORALIE
56749.987206	18.45	0.12	CORALIE
56749.993907	18.40	0.12	CORALIE
56750.987012	18.73	0.12	CORALIE
56750.993713	18.78	0.12	CORALIE
56825.955373	19.75	0.12	CORALIE
56825.962074	19.67	0.12	CORALIE
56826.952059	17.88	0.12	CORALIE
56826.958703	17.92	0.12	CORALIE
57134.970601	17.21	0.12	CORALIE
57135.972656	21.18	0.11	CORALIE
57136.971725	30.66	0.12	CORALIE
56213.389964	16.37	0.12	HARPS
56240.372796	26.41	0.12	HARPS
56242.391438	21.43	0.13	HARPS
56448.036297	31.24	0.13	HARPS
56450.018720	16.99	0.13	HARPS
56605.358090	31.18	0.13	HARPS
56606.176535	18.93	0.12	HARPS
56910.399809	21.31	0.13	HARPS